

Institute of Cybernetics at Tallinn University of Technology

Centre for Nonlinear Studies

**Propagation of $sech^2$ -type solitary waves
in higher order KdV-type systems**

Olari Ilison and Andrus Salupere

Research Report Mech 257/04

**Tallinn
2004**

Content

1. INTRODUCTION.....	3
2. STATEMENT OF THE PROBLEM.....	3
3. NUMERICAL METHOD	4
4. NUMERICAL RESULTS AND DISCUSSION.....	5
4.1. SOLUTION TYPES	6
4.1.1. <i>First type</i>	6
4.1.2. <i>Second type</i>	6
4.1.3. <i>Third type</i>	7
4.2. DISCUSSION	8
5. CONCLUSIONS	9
6. TABLES.....	10
7. FIGURES.....	13
8. REFERENCES.....	30

Abstract. Wave propagation in microstructured media is essentially influenced by nonlinear and dispersive effects. The simplest model governing these effects results in the Korteweg-de Vries (KdV) equation. In the present paper a KdV-type evolution equation, including the third- and fifth order dispersive and the fourth order nonlinear terms, is used for modelling the wave propagation in microstructured solids like martensitic-austenitic alloys. The model equation is solved numerically under localised initial conditions. Possible solution types are defined and discussed. It is shown that the relatively small solitary waves decay in time. However, if the amplitude exceeds a certain critical value then such a solitary wave can propagate with nearly a constant speed, amplitude and consequently the energy. Unlike the KdV solitons, interaction of such solitary waves is not perfectly elastic — after the interaction their speed and amplitude are altered by a small extent.

1. Introduction

Wave propagation in microstructured media is essentially influenced by nonlinear and dispersive effects. The simplest model governing these two effects results in the celebrated KdV equation

$$u_t + uu_x + du_{xxx} = 0. \quad (1)$$

However, studies of microstructured materials have shown that higher-order dispersive effects together with higher-order nonlinear effects can give rise to dramatic changes in the behaviour of emerging waves. In the present paper a KdV-like evolution equation, including the third- and the fifth order dispersive and the fourth order nonlinear terms,

$$u_t + [P(u)]_x + du_{xxx} + bu_{xxxxx} = 0 \quad (2)$$

is used for modelling the 1D longitudinal wave propagation in microstructured solids. Here u is the excitation, t the time coordinate, x the space coordinate, d and b the third- and the fifth-order dispersion parameters, respectively and elastic potential

$$P(u) = \left(-\frac{u^2}{2} + \frac{u^4}{4}\right), \quad (3)$$

introduces the quartic nonlinearity. The sources of higher order effects can be dislocations in the crystal structure of martensitic-austenitic shape-memory alloys (Maugin 1993, Maugin and Christov 1997).

The character of dispersion depends on the signs of parameters d and b . For $db < 0$ one has normal dispersion, however for $db > 0$ the dispersion is normal for some wavenumbers and anomalous for others (Salupere et al. 2001). In the present paper the normal dispersion case $d > 0$ and $b < 0$ is considered.

In Section 2 the problem is stated and in Section 3 the numerical method is described shortly. Results are presented and discussed in Section 4 and concluding remarks are given in Section 5. Tables and figures are presented in Sections 6 and 7, respectively.

2. Statement of the problem

The proposed model equation is solved numerically under localised initial conditions

$$u(x,0) = A \operatorname{sech}^2 \frac{x}{\Delta}, \quad (4)$$

where A is the amplitude and

$$\Delta = \sqrt{\frac{12d}{A}} \quad (5)$$

the width of the initial solitary wave (Zabusky and Kruskal 1965). In fact, the proposed localised initial excitation (4) corresponds to the analytical solution of the KdV equation (1). In our case the model equation (2) and the initial excitation (4) are related through the dispersion parameter d .

Logarithmic dispersion parameters

$$d_l = -\log d \quad \text{and} \quad b_l = -\log(-b) \quad (6)$$

are used instead of d and b for analysis herein after. Note that dispersion parameters have opposite sign in the present case, i.e. the normal dispersion case is studied here. In order to demonstrate the qualitative difference of dispersive terms in $b < 0$ and $b > 0$ cases quantities $du_{3x}(x,0)$ and $bu_{5x}(x,0)$ that correspond to the initial excitation (4) are presented in Figs. 1 and 2.

Boundary conditions are considered to be periodic, i.e.

$$u(x,t) = u(x + 4n\pi, t), \quad n = \pm 1, \pm 2, \dots, \quad (7)$$

because the pseudospectral method (described shortly in next Section) is applied for numerical integration of the problem (2)–(4). In order to separate localised initial waves the length of the space period in (7) was taken 4π .

Goals of the current study are

- (i) to find numerical solutions for the proposed problem over wide range of logarithmic dispersion parameters d_l and b_l ;
- (ii) to examine and describe the time-space behaviour of numerical solutions;
- (iii) to introduce solution types. Our particular interest is to examine whether or not solitary waves (4) can propagate in media described by the equation (2) with constant speed and amplitude. Furthermore, pilot study is carried out in order to understand how such solitary waves interact in such a media. In the other words, do the solitary waves (4) behave like solitons in media where the higher order effects, governed by the equation (2), are of importance.

3. Numerical method

Based on previous experience the pseudospectral method (PsM) (Fornberg 1998, Salupere 1995, Salupere 1997) is used for numerical integration of the model equation (2) under localised initial conditions (4) and periodic boundary conditions (7), i.e., for the numerical simulation of wave propagation in media described by the KdV-like evolution equation (2). Results are analysed using discrete spectral characteristics (Salupere et al. 1996).

The pseudospectral method was first proposed by Kreiss and Oliger (1972) in the following form. Let the initial condition $u(x,0)$ be given on the interval 2π . The space grid is formed by n points with

$$\Delta x = \frac{2\pi}{n}. \quad (8)$$

The discrete Fourier transform (DFT) is defined by

$$U(\omega, t) = Fu = \sum_{j=0}^{n-1} u(j\Delta x, t) e^{\left(\frac{-2\pi j\omega}{n}\right)} \quad (9)$$

and the inverse discrete Fourier transform (IDFT) by

$$u(x, t) = F^{-1}U = \sum_{\omega} U(\omega, t) e^{\left(\frac{2\pi j\omega}{n}\right)} \quad (10)$$

where i is the imaginary unit and

$$\omega = 0, \pm 1, \pm 2, \dots, \pm\left(\frac{n}{2}-1\right), -\frac{n}{2}. \quad (11)$$

In expressions (9) and (10) F denotes the Fourier transform and F^{-1} the inverse Fourier transform. Fast Fourier Transform (FFT) algorithm is applied to find the Fourier transform (Bracewell 1972). Space derivatives are then given by

$$\begin{aligned}\frac{\partial u}{\partial x} &= F^{-1}(i\omega F), \\ \frac{\partial^2 u}{\partial x^2} &= -F^{-1}(\omega^2 Fu), \\ &\dots\end{aligned}\tag{12}$$

$$\frac{\partial^n u}{\partial x^n} = F^{-1}[(i\omega)^n Fu].$$

In time, the finite difference leap-frog (LF) scheme was proposed to use by Kreiss and Olinger (1972). For example, the KdV-like equation (2) with quartic potential (3) leads to the following straightforward pseudospectral approximation

$$u(x, t + \Delta t) = u(x, t - \Delta t) - 2\Delta t(u^3 - u)F^{-1}(i\omega Fu) + 2d\Delta tF^{-1}(i\omega^3 Fu) - 2b\Delta tF^{-1}(i\omega^5 Fu).\tag{13}$$

The LF scheme has a disadvantage. Namely, one has to use very small time step to get stable results. Furthermore, there are not proper criterions for choosing suitable (in the sense of stability of the numerical scheme) size for the time step. Runge-Kutta type methods are found to be more stable than LF scheme. Hence, the step-size controlling Runge-Kutta-Fehlberg (RKF) algorithm is used in numerical experiments below (Salupere 1997).

For future analysis spectral amplitudes are defined as:

$$S_\omega(t) = \frac{2|U(\omega, t)|}{N}, \quad \omega = 1, \dots, \frac{N}{2}.\tag{14}$$

The variable $U(\omega, t)$ is given by the DFT expression (9). These spectral characteristics carry additional information about the internal structure of waves. This information is related to the existence of local and global minima and maxima in time dependence of spectral curves.

4. Numerical results and discussion

The problem (2)–(4) is solved numerically over the range of the dispersion parameters

$$0.8 \leq d_l \leq 2.4 \quad \text{and} \quad 1.2 \leq b_l \leq 4.8\tag{15}$$

in order to examine different properties of the solutions. The length of the integration interval and the time-step for saving of results, t_f and Δt respectively, were chosen according to the nature of solutions. The number of space-grid points was varied ($n = 64, 128, 256, 512$) accordingly to the behaviour of densities

$$C_1 = \int_0^{4\pi} u dx, \quad C_2 = \int_0^{4\pi} u^2 dx\tag{16}$$

of the first two conservation laws. In the other words, the number of space-grid points was kept as low as possible and the criterion was that relative error for density C_2 must be less than 0.005.

4.1. Solution types

By making use of numerical results one can detect that the type of the solution depends on the value of the amplitude A essentially. Generally speaking one can find three different solution types. Two of those types can be detected for all values of dispersion parameters d_l and b_l in the considered domain (15), whereas one solution type was detected only in a certain sub domain, i.e., only for few values of dispersion parameters.

4.1.1. First type

The first solution type can be described as a chaotic spread of initial energy, i.e., the localised initial excitation falls apart into a chaotic train of waves (Figs. 3-5).

- One cannot detect any regularity neither in the time-space behaviour of wave-profile characteristics (time dependences of wave-profile minima and maxima and their trajectories nor in time dependences of spectral amplitudes (Figs. 6-8)).
- This phenomenon (the formation of the chaotic wave-train) can be explained as a shortage of initial energy to form a single wave profile, which can propagate in the considered media with constant speed and shape, i.e., conserving its initial energy.

4.1.2. Second type

The second solution type can be detected if the initial wave amplitude A exceeds a certain value $A_1(d_l, b_l)$. In this case a wave-train having periodic behaviour in time emerges.

- Periodicity can be detected in the time-space behaviour of wave-profile characteristics as well as in time dependences of spectral amplitudes (Figs. 9-12).
- One can detect that wave profiles are stretched to the positive as well as to the negative direction. For certain time intervals positive and for another time intervals negative solitary waves can be detected. (see Figs. 13 and 14).
- Furthermore, these solitary waves have solitonic behaviour — they restore their shape and speed throughout interactions.
- By making use of time dependences of spectral amplitudes one can detect the recurrence and super-recurrence phenomena, i.e., after a certain time interval t_R the initial (spectral) state is almost restored (see Figs. 11 and 12). If the k -th recurrence is better than the first, then the k -th recurrence is called the super-recurrence like in the case of the KdV equation (Goda 1977, Abe and Abe 1979).
- Common feature for the first and the second type of the solutions is that negative solitary wave can be seen during time frame where first spectral amplitude has the steepest slope (see Fig 15).

4.1.3. Third type

If the initial wave amplitude has values over a certain critical value $A^*(d_l, b_l)$ then the initial excitation propagates with minimal disturbances, i.e., its speed, amplitude and consequently the energy changes by a small extent only during the propagation. Lower and upper limit, A^l and A^u respectively, for the critical amplitude $A^*(d_l, b_l)$ are presented against logarithmic dispersion parameters d_l and b_l in Table 1. If the amplitude of the initial solitary wave $A = A^l$ then the solution is of the first or the second type. However, if $A = A^u$ then the one has the third type of solution. The difference between lower and the upper limit $A^u - A^l = 0.01$, i.e., the critical amplitude is determined with the accuracy 0.01. Notice, that the determination of such critical amplitude was one of the main goals of the present study.

- The higher the amplitude (for fixed values of d_l and b_l) of the initial wave the higher its speed (Figs. 16-19 and Tables 2-7).
- Besides the solitary wave (propagating to the right) left propagating (relatively) small amplitude oscillating wave-train forms. For all considered pairs of logarithmic dispersion parameters d_l and b_l there exist the initial solitary wave amplitude A_{best} where the amplitude of the oscillating wave-train is the smallest for this particular set of dispersion parameters (Figs. 20-21). It is convenient to use spectral amplitudes in order to estimate the alteration of the solitary wave during the propagation. The maximum deviation of k -th spectral amplitude is defined as $\Delta_{S_k} = S_{k \max} - S_{k \min}$ where $S_{k \max} = \max_t S_k(t)$ and $S_{k \min} = \min_t S_k(t)$ are the maximum and the minimum value of the k -th spectral amplitude over the considered time interval. It is clear that $\Delta_{S_k} > 0$ and the smaller the deviation Δ_{S_k} the smaller are the mutations of the solitary wave during the propagation. In Table 8 the smallest value of the deviation Δ_{S_k} and corresponding initial wave amplitude A_{best} are presented against logarithmic dispersion parameters d_l and b_l . In some cases $A_{best} = A^u(d_l, b_l)$ (for example the case $d_l=0.8$ and $b_l=4.8$; $d_l=1.2$ and $b_l=3.6$), however in some cases $A_{best} > A^u(d_l, b_l)$ (for example in the case $d_l=2.4$ and $b_l=4.0$). The higher the value of the initial wave amplitude in the domain $A > A_{best}$ the higher the value of Δ_{S_k} and the more distinctive the left propagating wave-train.
- The amplitude of the solitary wave oscillates by a small extent during the propagation. In some cases the solitary wave amplitude oscillates near the initial amplitude A , however in some cases at first the amplitude rises (or falls) during a short time interval and then starts to oscillate around a certain value higher (or lower) than the initial amplitude A (see Figs. 22-25).
- It is complicated to establish direct relations between the time-space behaviour of the solitary wave and time dependences of spectral amplitudes S_i ($i = 1, 2, 3, \dots$) in the case of the third solution type. In some cases different spectral amplitude curves intersect, but in some cases they are separated, notwithstanding that in both cases a solitary wave propagates at nearly constant speed and amplitude. However, common features of time dependences of spectral amplitudes are (i) that the lower order spectral

amplitudes dominate over that of the higher order and (ii) (quasi)periodic behaviour (see Figs. 26-27).

4.2. Discussion

In the considered domain of dispersion parameters (15) there exist sub domains where the third order dispersive effects dominate over that of the fifth order and, vice versa, sub domains where the fifth order dispersive effects dominate over that of the third order. We say that fifth order dispersive effects are dominating over these of the third order if

$$r_d = \frac{\max_x |bu_{5x}(x,0)|}{\max_x |du_{3x}(x,0)|} > 10, \quad (17)$$

and *vice versa*, third order dispersive effects are dominating if

$$r_d = \frac{\max_x |bu_{5x}(x,0)|}{\max_x |du_{3x}(x,0)|} < 0.1. \quad (18)$$

The ratio r_d depends on the value of the amplitude of the initial wave A as well as on dispersion parameters d and b . In Fig. 28 the ratio r_d is presented against logarithmic dispersion parameters d_l and b_l in the form of contour lines for values $A=1.6$ and $A=2.8$ (the critical amplitude $1.6 < A^* < 2.8$ in numerical experiments, see Table 1). The presented contour lines can be approximated by straight lines $b_l = 2d_l + D$, where the constant D is defined by parameters d_l and b_l . For fixed values of d_l^* and b_l^* constant $D^* = b_l^* - 2d_l^*$.

In Fig. 29 lower limits A^l (detected in numerical experiments) for critical amplitude A^* are presented. One can conclude that along lines $b_l = 2d_l + D$ the value of A^l deviates by a small extent $\Delta A = \pm 0.01$. In other words, quantity $b_l - 2d_l$ determines the value the lower limit A^l and therefore the value of the critical amplitude A^* as well.

In Fig. 30 the ratio r_d is presented against logarithmic dispersion parameters d_l and b_l for $A = A^l$. It is clear that for $A=2.71$ the ratio $r_d > 10$ and fifth order dispersive effects are dominating and for $A \leq 1.69$ the ratio $r_d < 0.1$ and third order dispersive effects are dominating. Our particular interest is paid to the case when neither third nor fifth order dispersive effects are dominating, i.e. the amplitude of the initial wave $1.69 < A < 2.71$. The latter is determined by values $-0.8 < b_l - 2d_l < 1.6$.

In addition to the results presented in Table 1 lower and upper limits, A^l and A^u respectively, for critical amplitude A^* were found for four pairs of dispersion parameters outside of the initial set of values. The results were in accordance with previous experiments — $1.77 < A^* < 1.78$ for $d_l=0.8$ and $b_l=2.4$; $1.77 < A^* < 1.78$ for $d_l=1.2$ and $b_l=3.2$; $2.02 < A^* < 2.03$ for $d_l=1.2$ and $b_l=2.4$; $2.02 < A^* < 2.03$ for $d_l=1.6$ and $b_l=3.2$.

In Fig. 31 values of the lower limit A^l are plotted against $b_l - 2d_l$. Discrete values correspond to numerical experiments and solid line to the eighth order polynomial interpolation.

In the case of KdV equation the amplitude and speed of the solution are directly related: $A/c = 3$. In the studied case, i.e. in the case of KdV435 equation, there doesn't exist such a

fixed ratio. In Tables 2–7 the location of solitary wave maximum x_M ($u(x_M, t) = \max_x u(x, t)$), displacement $\Delta x(t) = x_M(t) - x_M(0)$, the average speed $c = \Delta x/t$ and the ratio A/c are presented against time for different values of d_l , b_l and A . One can only conclude that the higher the amplitude A the greater the solitary wave speed and the smaller the ratio A/c .

Computations were carried out for modelling interaction between two solitary waves in order to test the solitonic character of the third type solutions. For simulation of interaction two third-type of solutions having different amplitudes were chosen ($A_1 = 2.73$, $A_2 = 2.90$ for $d_l=1.6$, $b_l=2.8$ and $A_1 = 2.08$, $A_2 = 2.12$ for $d_l=2.4$, $b_l=4.8$). Due to the difference in solitary waves' amplitudes, solitary wave with higher amplitude (and speed, respectively) starts to catch up solitary wave with lower amplitude (see Figs. 32 and 33). Analysis of numerical results (solitary wave trajectories and amplitudes were traced) shows that the interaction of these two solitary waves is close to the typical behaviour of solitons — both solitary waves almost restore their speed and amplitude after interaction. However, a certain alteration of solitary wave shape and speed (and therefore the energy) exists, so one can not name this kind of interaction perfectly elastic.

5. Conclusions

In the present paper the propagation of $a \operatorname{sech}^2 bx$ type localised initial wave (KdV soliton) in media characterised by higher order nonlinearity and higher order dispersion is studied. Main attention is paid to the case when neither the third- nor the fifth order dispersive effects are dominating. As main results the following can be drawn out:

- Three solution types are detected.
- In the case of the first type the initial solitary wave (4) is spread into a train of waves having chaotic (irregular) space-time behaviour.
- In the case of the second type the initial solitary wave is destroyed as well. However, one can clearly distinct positive and negative solitary waves in the formed wave-train now. Furthermore, (quasi)periodic behaviour (including the recurrence and superrecurrence phenomena) can be detected in time dependences of spectral amplitudes.
- If the amplitude A exceeds a certain threshold A^* then the initial solitary wave (4) can travel with a constant speed and without significant changes in its amplitude. This case is referred as the third solution type.
- Numerical experiments with solitary waves having different amplitudes (and therefore different speeds) demonstrate that their interaction is not perfectly elastic — there exist a certain small transformation of energy and/or mass between interacting solitons. This phenomenon causes the slower solitary wave move more slowly and the faster one even faster.

6. Tables

Table.1. Lower and upper limits ($A^l - A^u$) for the critical amplitude A^* depending on values of dispersion parameters d_l and b_l .

b_l					
	$d_l = 0.8$	$d_l = 1.2$	$d_l = 1.6$	$d_l = 2.0$	$d_l = 2.4$
1.2	2.27-2.28				
2.0	1.86-1.87	2.27-2.28			
2.8	1.72-1.73	1.87-1.88	2.28-2.29		
3.6	1.67-1.68	1.72-1.73	1.87-1.88	2.28-2.29	
4.0	1.67-1.68	1.69-1.70	1.78-1.79	2.02-2.03	2.71-2.72
4.4	1.67-1.68	1.68-1.69	1.73-1.74	1.87-1.88	2.28-2.29
4.8	1.67-1.68	1.68-1.69	1.69-1.70	1.78-1.79	2.02-2.03

Table.2. Third solution type. Location of the solitary wave maximum x_M , corresponding displacement Δx , speed c , and amplitude-speed ratio A/c against time t . Case $d_l=2.0$ and $b_l=4.0$, $A=2.03$.

t	x_M	Δx	c	A/c
0	6.2382			
10	7.7558	1.4726	0.1428	14.2157
20	9.0321	2.7489	0.1375	14.7636
30	10.2102	3.9270	0.1324	15.3323
40	11.3883	5.1051	0.1276	15.9091

Table.3. Third solution type. Location of the solitary wave maximum x_M , corresponding displacement Δx , speed c , and amplitude-speed ratio A/c against time t . Case $d_l=2.0$ and $b_l=4.0$, $A=2.09$.

t	x_M	Δx	c	A/c
0	6.2382			
10	9.7193	3.4361	0.3436	6.0827
20	13.1554	6.8722	0.3436	6.0827
30	16.6897	10.4065	0.3469	6.0248
40	20.1258	13.8426	0.3461	6.0387

Table.4. Third solution type. Location of the solitary wave maximum x_M , corresponding displacement Δx , speed c , and amplitude-speed ratio A/c against time t . Case $d_I=1.6$ and $b_I=2.8$, $A=2.29$.

t	x_M	Δx	c	A/c
0	6.2382			
10	8.1485	1.8653	0.1865	12.2788
20	9.6211	3.3379	0.1669	13.7208
30	11.094	4.8106	0.1604	14.2768
40	12.468	6.1850	0.1546	14.8124

Table.5. Third solution type. Location of the solitary wave maximum x_M , corresponding displacement Δx , speed c , and amplitude-speed ratio A/c against time t . Case $d_I=1.6$ and $b_I=2.8$, $A=2.34$.

t	x_M	Δx	c	A/c
0	6.2382			
10	9.6211	3.3379	0.3379	6.9251
20	12.9591	6.7209	0.3360	6.9643
30	16.1988	9.9606	0.3320	7.0482
40	19.6350	13.3968	0.3349	6.9872

Table.6. Third solution type. Location of the solitary wave maximum x_M , corresponding displacement Δx , speed c , and amplitude-speed ratio A/c against time t . Case $d_I=0.8$ and $b_I=4.8$, $A=1.68$.

t	x_M	Δx	c	A/c
0	6.2382			
10	7.5595	1.2763	0.1276	13.1661
20	9.7193	3.4361	0.1718	9.7788
30	13.352	7.0686	0.2356	7.1307
40	15.315	9.0321	0.2258	7.4402

Table.7. Third solution type. Location of the solitary wave maximum x_M , corresponding displacement Δx , speed c , and amplitude-speed ratio A/c against time t . Case $d_I=0.8$ and $b_I=4.8$, $A=1.71$.

t	x_M	Δx	c	A/c
0	6.2382			
10	9.1303	2.8921	0.2892	5.9129
20	14.3335	8.0953	0.4048	4.2243
30	16.7879	10.5497	0.3517	4.8621
40	21.1076	14.8694	0.3717	4.6005

Table.8. Smallest values of deviation Δ_{s_k} and corresponding amplitude A against dispersion parameters d_l and b_l .

b_l					
	$d_l = 0.8$	$d_l = 1.2$	$d_l = 1.6$	$d_l = 2.0$	$d_l = 2.4$
1.2	0.0082 2.52				
2.0	0.0131 1.89	0.0026 2.49			
2.8	0.0598 1.73	0.0048 1.89	0.0028 2.48		
3.6	0.0641 1.68	0.0329 1.73	0.0047 1.89	0.0007 2.48	
4.0	0.1004 1.68	0.0724 1.70	0.0088 1.79	0.0005 2.09	0.0005 3.41
4.4	0.1128 1.68	0.0858 1.69	0.0371 1.74	0.0036 1.90	0.0006 2.47
4.8	0.1261 1.68	0.1054 1.69	0.0420 1.70	0.0044 1.79	0.00002 2.09

7. Figures

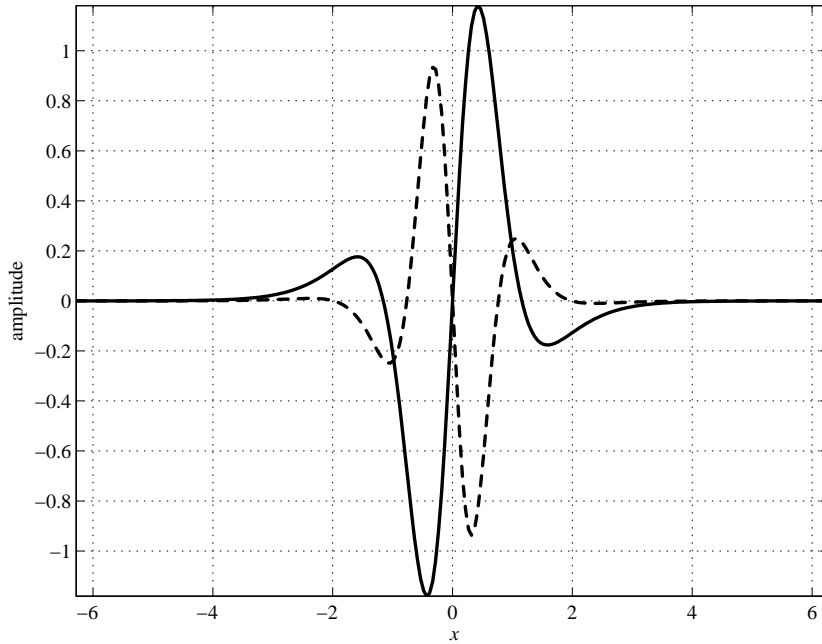


Fig. 1. Third- and fifth order dispersive terms of the initial wave profile, case $d_l=0.8$, $b_l=2.0$, $A=1.87$ and $b>0$ ($b_l = -\log b$). Solid line corresponds to the third- and dashed line to fifth-order term.

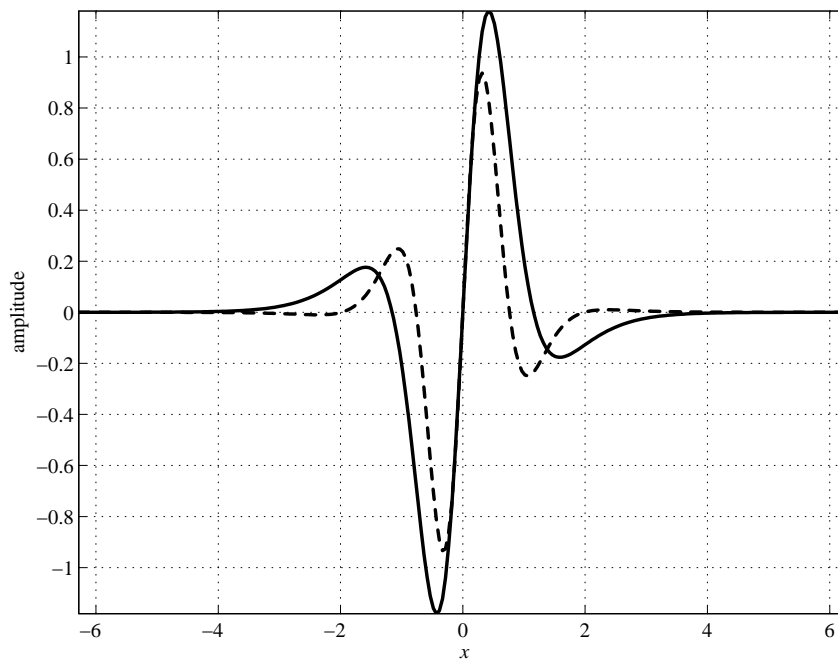


Fig. 2. Third- and fifth order dispersive terms of the initial wave profile, case $d_l=0.8$, $b_l=2.0$, $A=1.87$ and $b<0$ ($b_l = -\log(-b)$). Solid line corresponds to the third- and dashed line to fifth-order term.

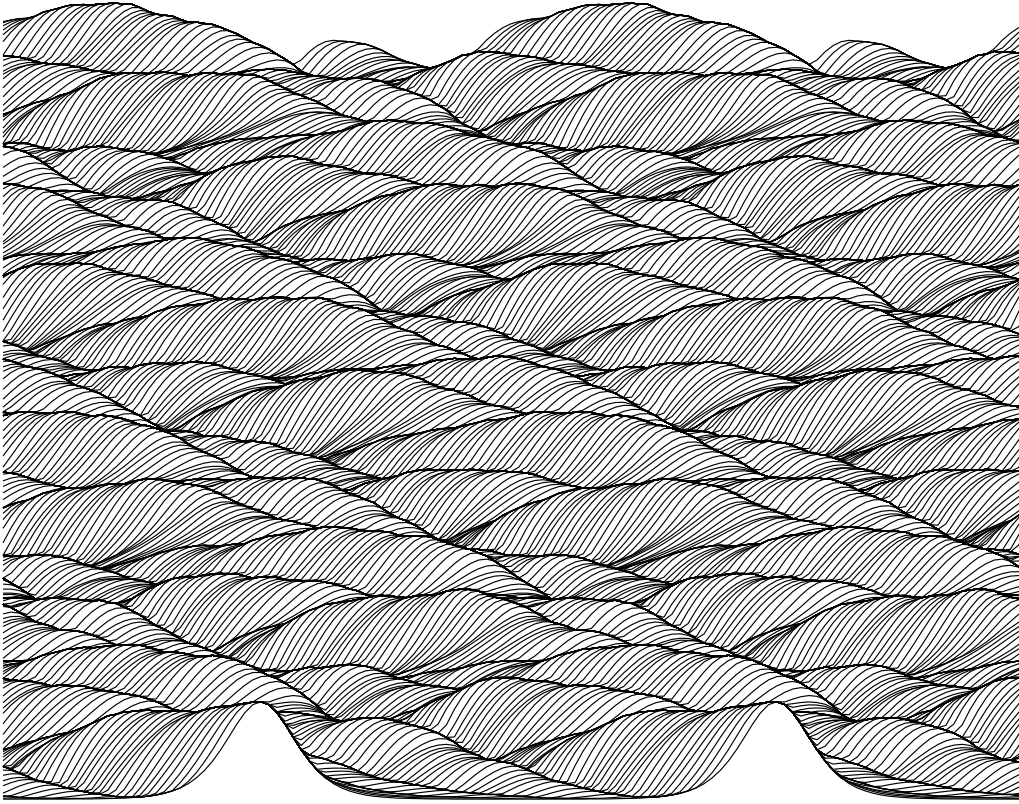


Fig. 3. First solution type. Propagation of initial excitation (4), amplitude $A=1.5$, $d_l=0.8$ and $b_l=2.0$ and $t_f=300$, $n=128$.

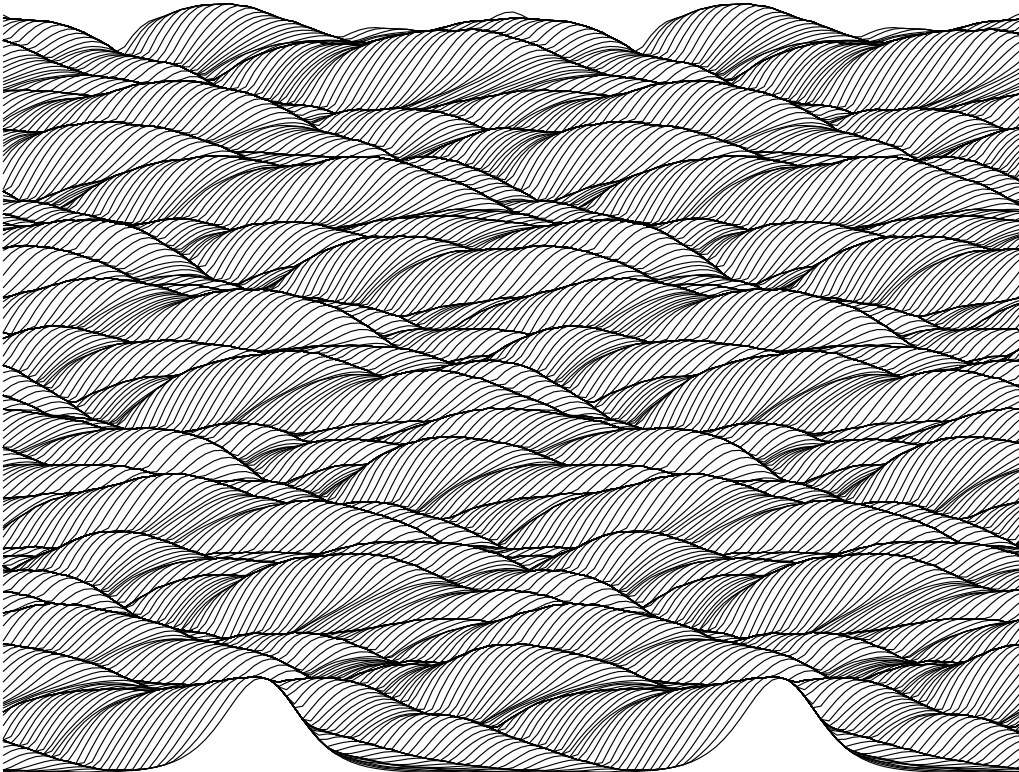


Fig. 4. First solution type. Propagation of initial excitation (4), amplitude $A=1.25$, $d_l=0.8$ and $b_l=4.8$ and $t_f=300$, $n=128$.

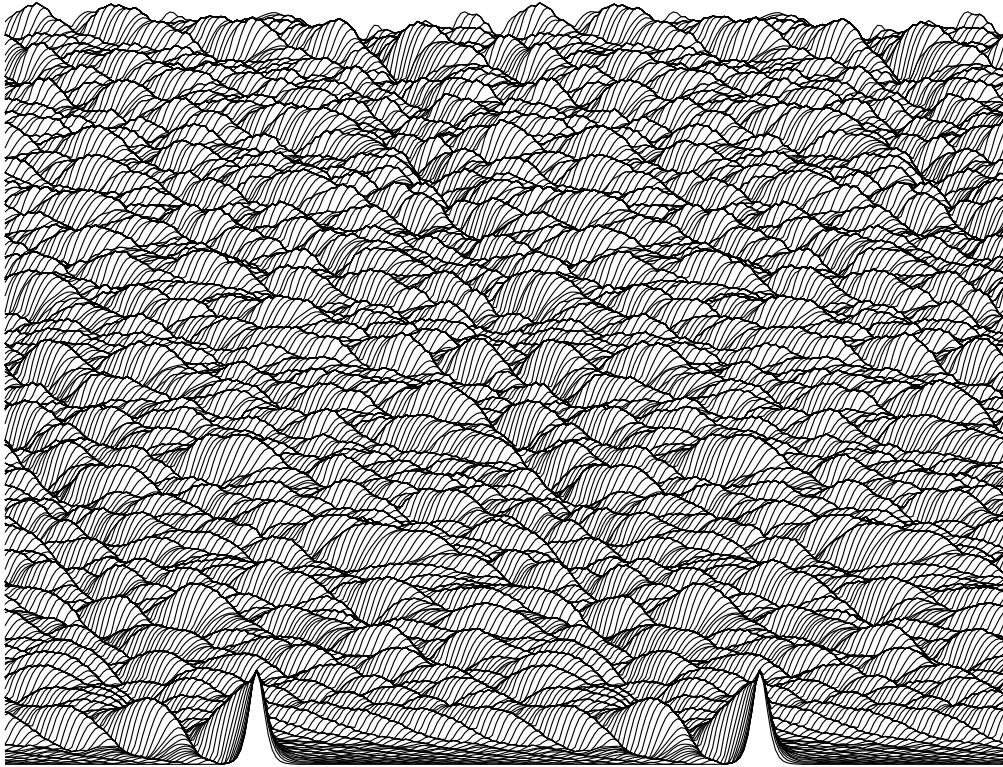


Fig. 5. First solution type. Propagation of initial excitation (4), amplitude $A=1.95$, $d_I=2.0$ and $b_I=4.0$ and $t_f=300$, $n=128$.

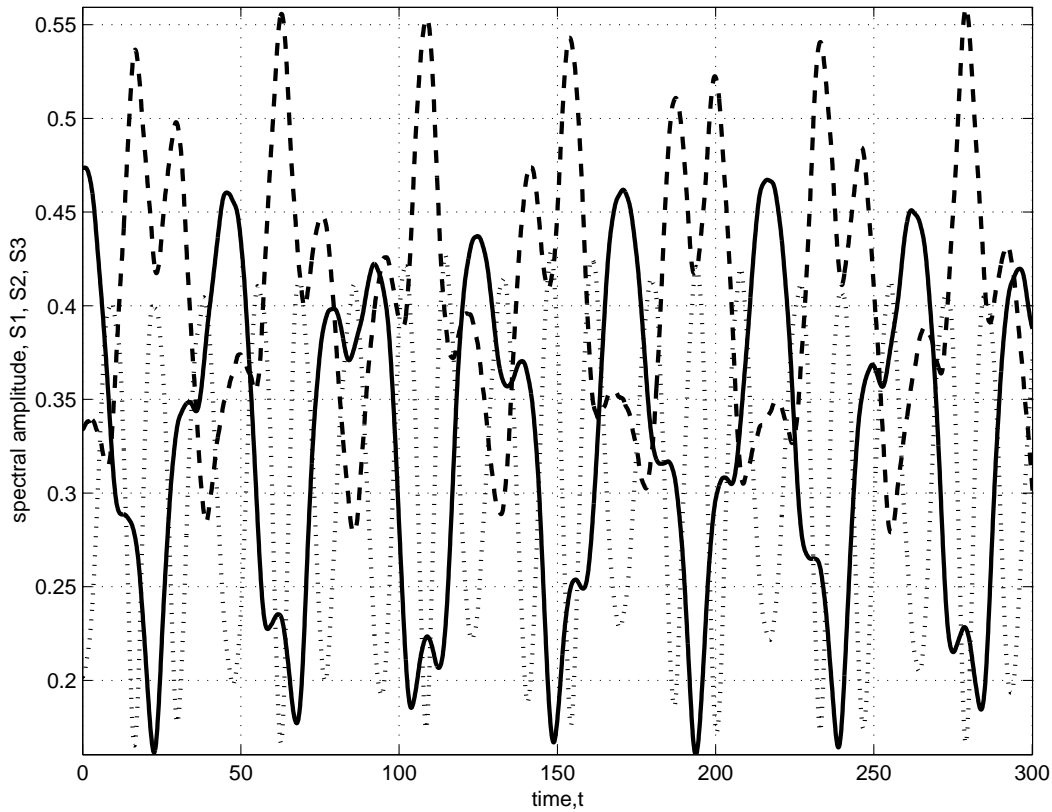


Fig. 6. First solution type. First three spectral amplitudes S_1 , S_2 , S_3 against time; case $A=1.50$, $d_I=0.8$ and $b_I=2.0$ (solid line corresponds to S_1 , dashed line to S_2 and dotted line to S_3).

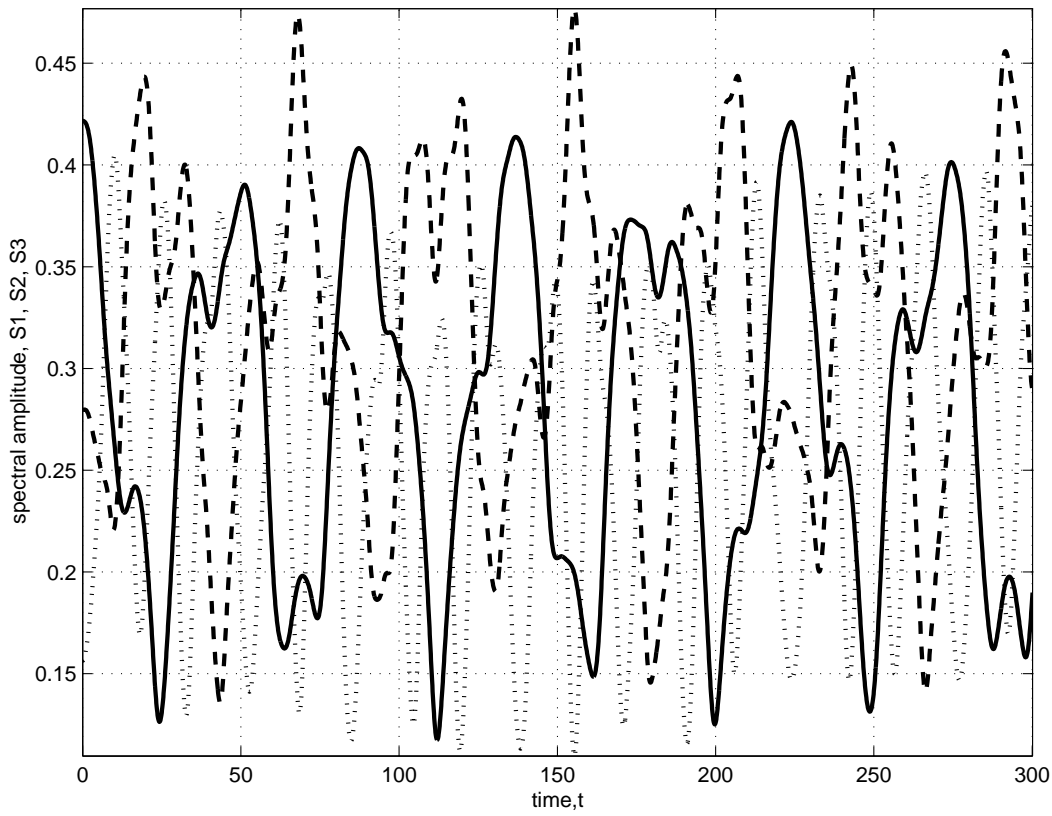


Fig. 7. First solution type. First three spectral amplitudes S_1 , S_2 , S_3 against time; case $A=1.25$, $d_1=0.8$ and $b_1=4.8$ (solid line corresponds to S_1 , dashed line to S_2 and dotted line to S_3).

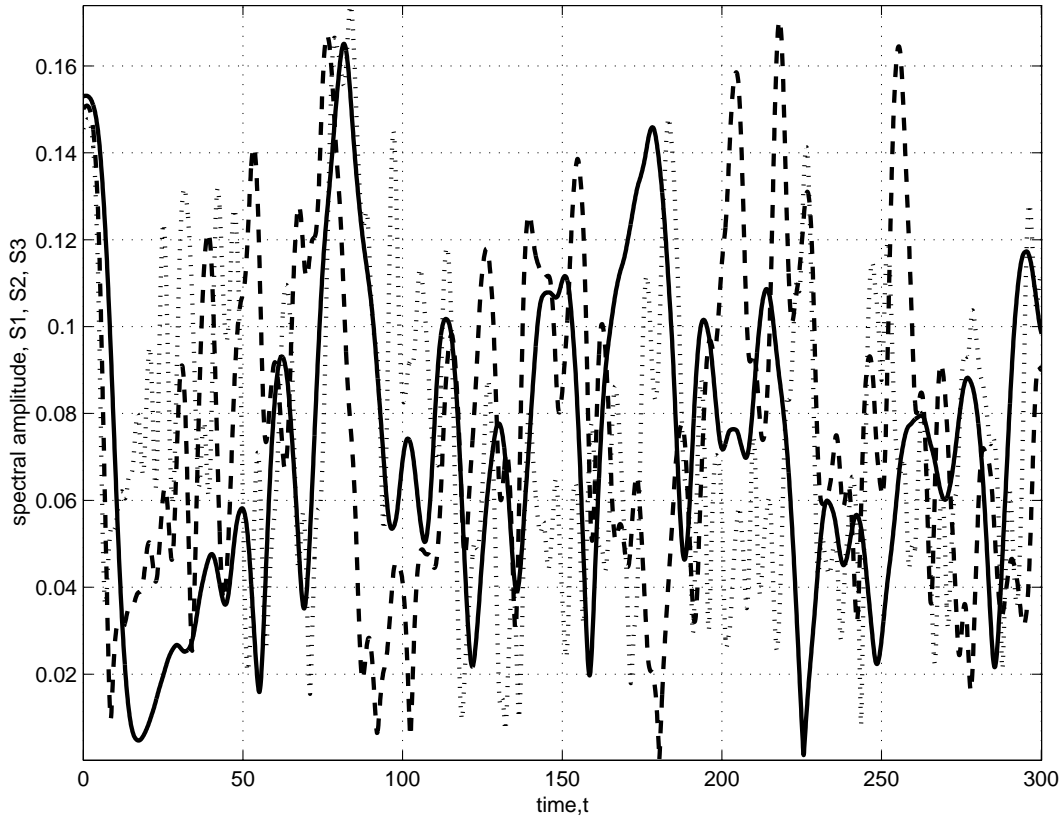


Fig. 8. First solution type. First three spectral amplitudes S_1 , S_2 , S_3 against time; case $A=1.95$, $d_1=2.0$ and $b_1=4.0$ (solid line corresponds to S_1 , dashed line to S_2 and dotted line to S_3).

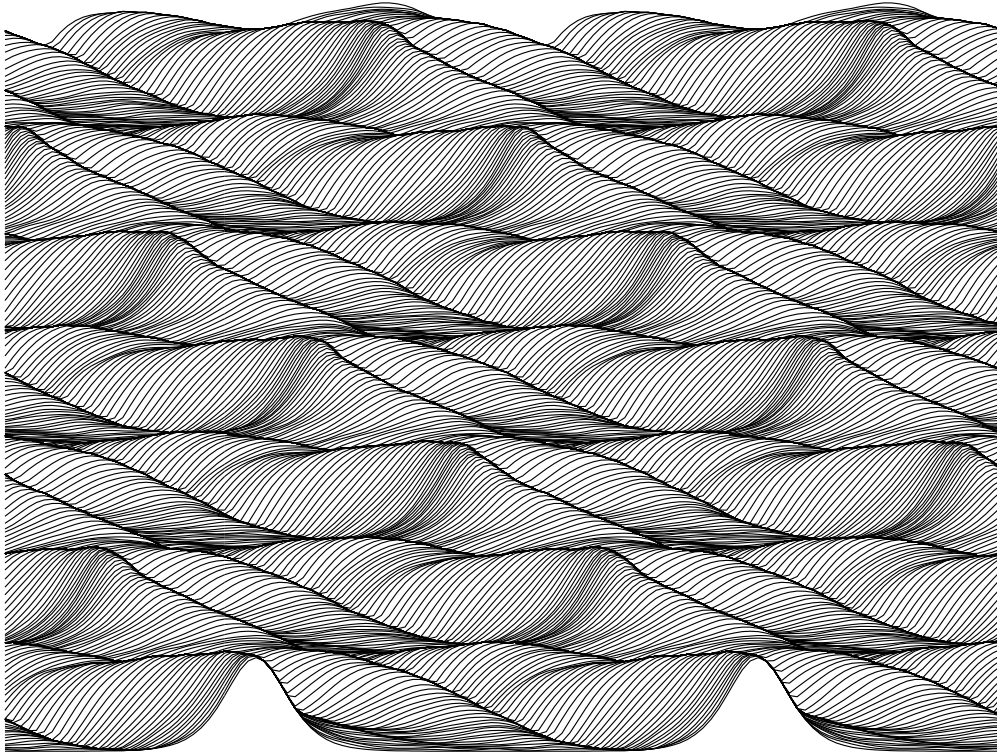


Fig. 9. Second solution type. Propagation of initial excitation (4), amplitude $A=1.75$, $d_1=0.8$ and $b_1=2.0$ and $t_f=300$, $n=128$.

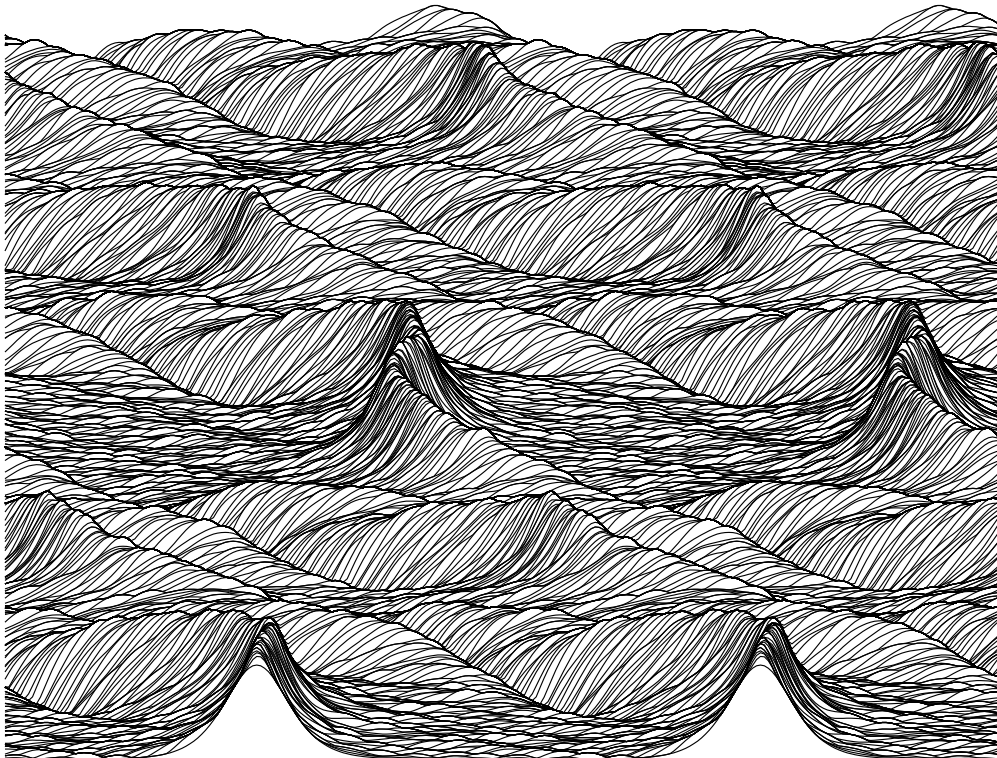


Fig. 10. Second solution type. Propagation of initial excitation (4), amplitude $A=1.66$, $d_1=0.8$ and $b_1=4.8$ and $t_f=300$, $n=128$.

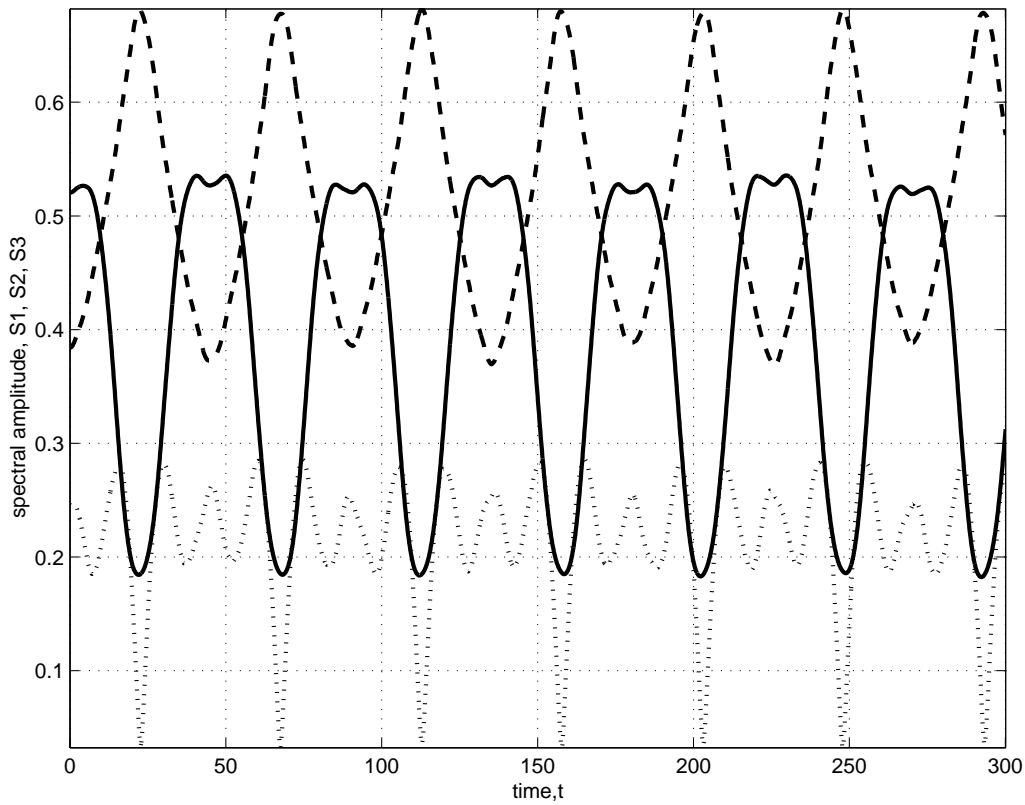


Fig. 11. Second solution type. First three spectral amplitudes S_1 , S_2 , S_3 against time; case $A=1.75$, $d_I=0.8$ and $b_I=2.0$ (solid line corresponds to S_1 , dashed line to S_2 and dotted line to S_3).

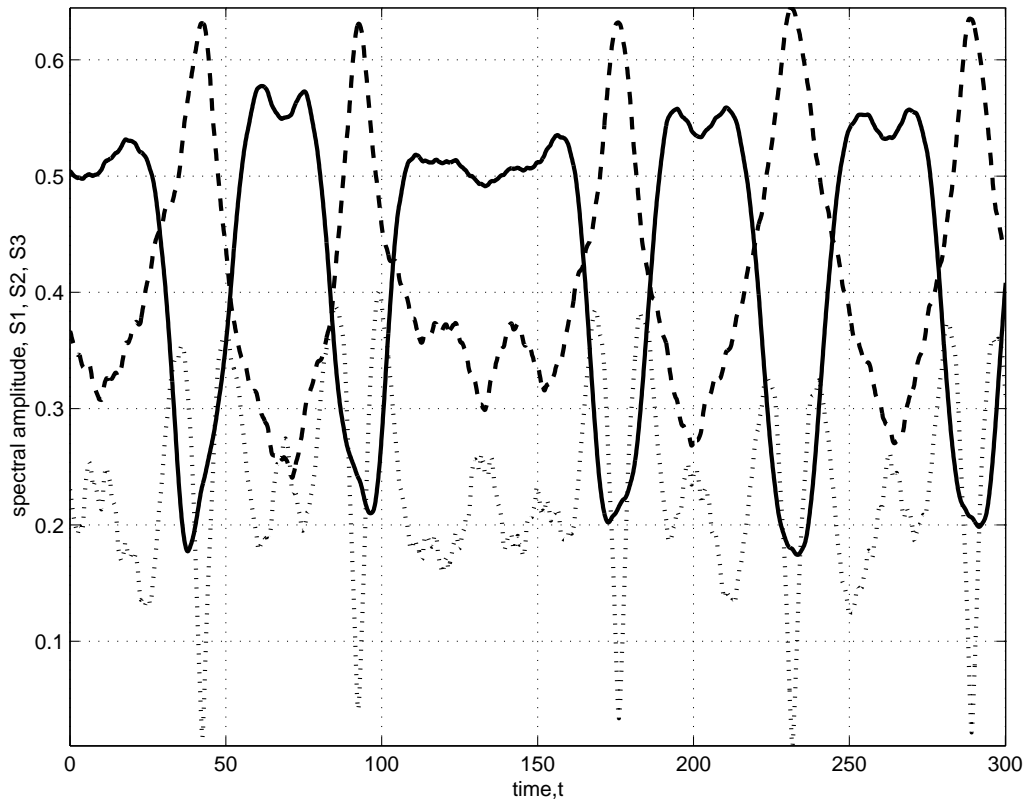


Fig. 12. Second solution type. First three spectral amplitudes S_1 , S_2 , S_3 against time; case $A=1.66$, $d_I=0.8$ and $b_I=4.8$ (solid line corresponds to S_1 , dashed line to S_2 and dotted line to S_3).

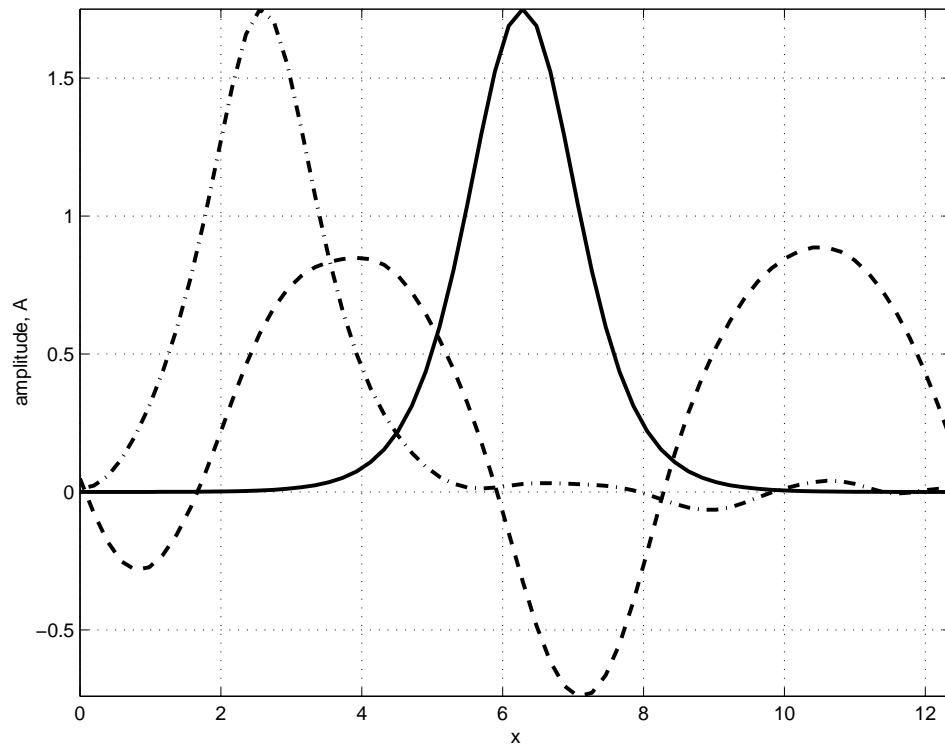


Fig. 13. Second solution type. Wave profiles of the solution, case $d_l=0.8$, $b_l=2.0$ and $A=1.75$. Solid line corresponds to time moment $t=0$, dash-dotted line corresponds to time moment $t=45.6$, dashed line corresponds to time moment $t=90.2$.

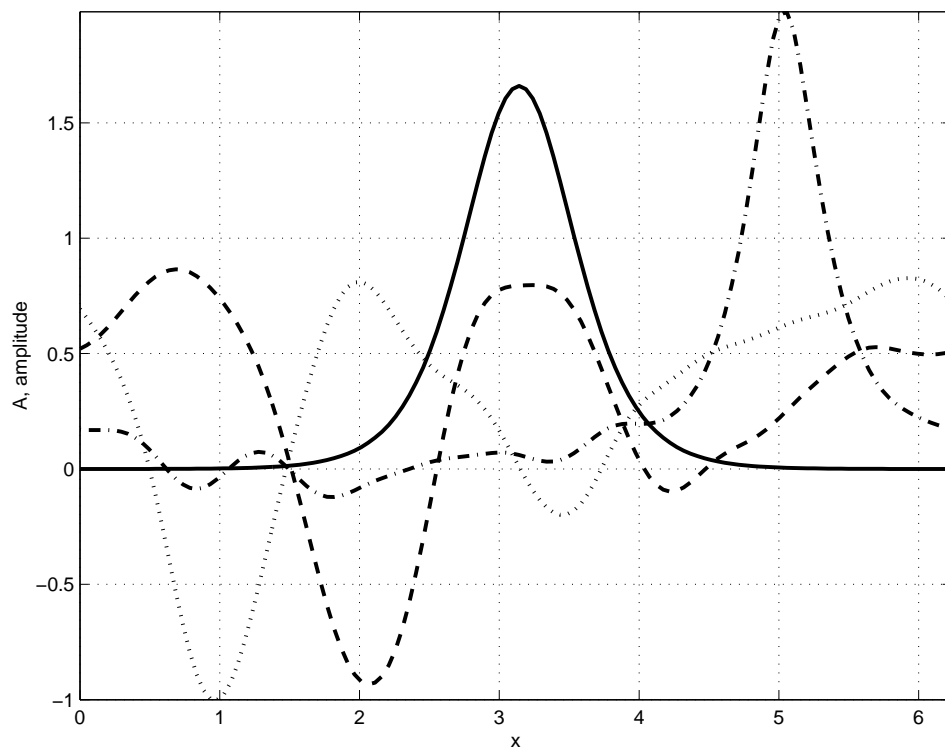


Fig. 14. Second solution type. Wave profiles of the solution, case $d_l=0.8$, $b_l=4.8$ and $A=1.66$. Solid line corresponds to time moment $t=0$, dashed line corresponds to time moment $t=99.3$, dash-dotted line corresponds to time moment $t=133.7$ and dotted line corresponds to time moment $t=296.5$.

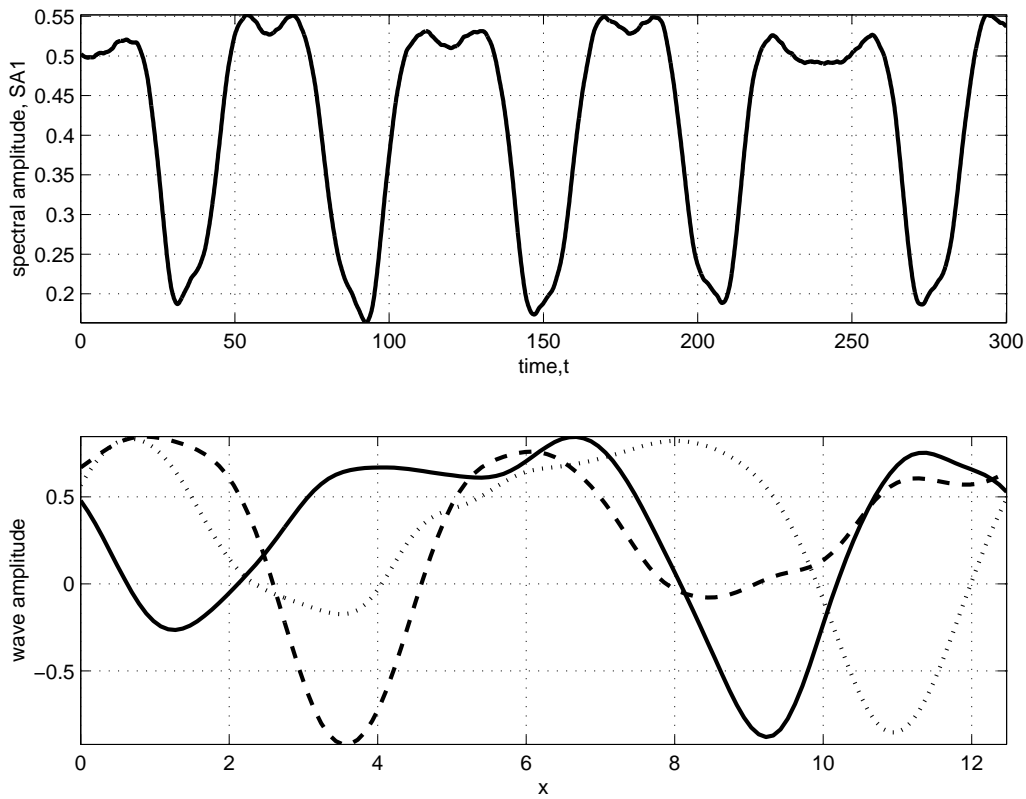


Fig. 15. Second solution type. First spectral amplitude S_1 and wave profiles of the solution, case $d_l=0.8$, $b_l=4.8$ and $A=1.65$. Solid line corresponds to time moment $t=41.6$, dashed line corresponds to time moment $t=96.0$ and dotted line corresponds to time moment $t=157$.

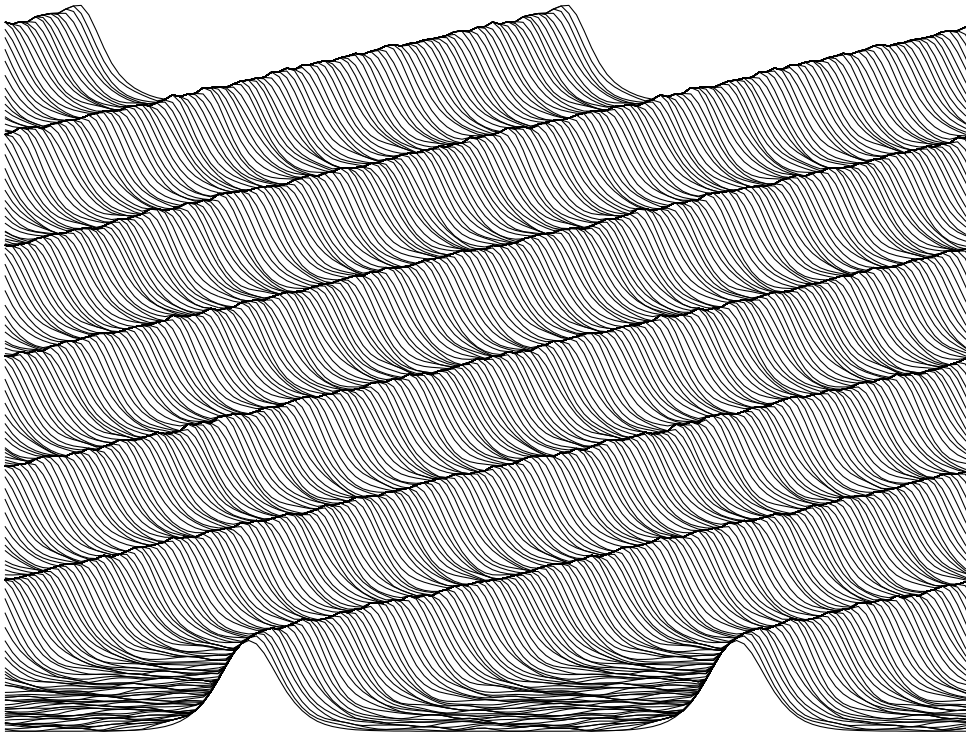


Fig. 16. Third solution type. Propagation of initial excitation (4), amplitude $A=1.90$, $d_l=0.8$ and $b_l=2.0$ and $t_f=300$, $n=128$.

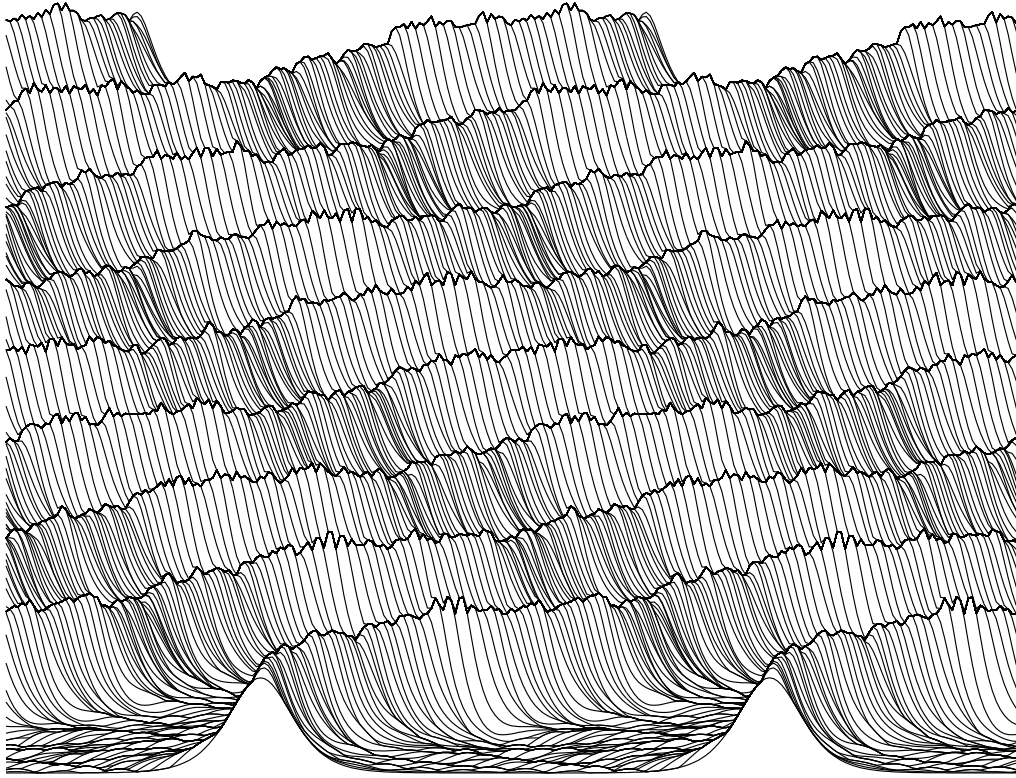


Fig. 17. Third solution type. Propagation of initial excitation (4), amplitude $A=1.70$, $d_I=0.8$ and $b_I=4.8$ and $t_f=300$, $n=128$.

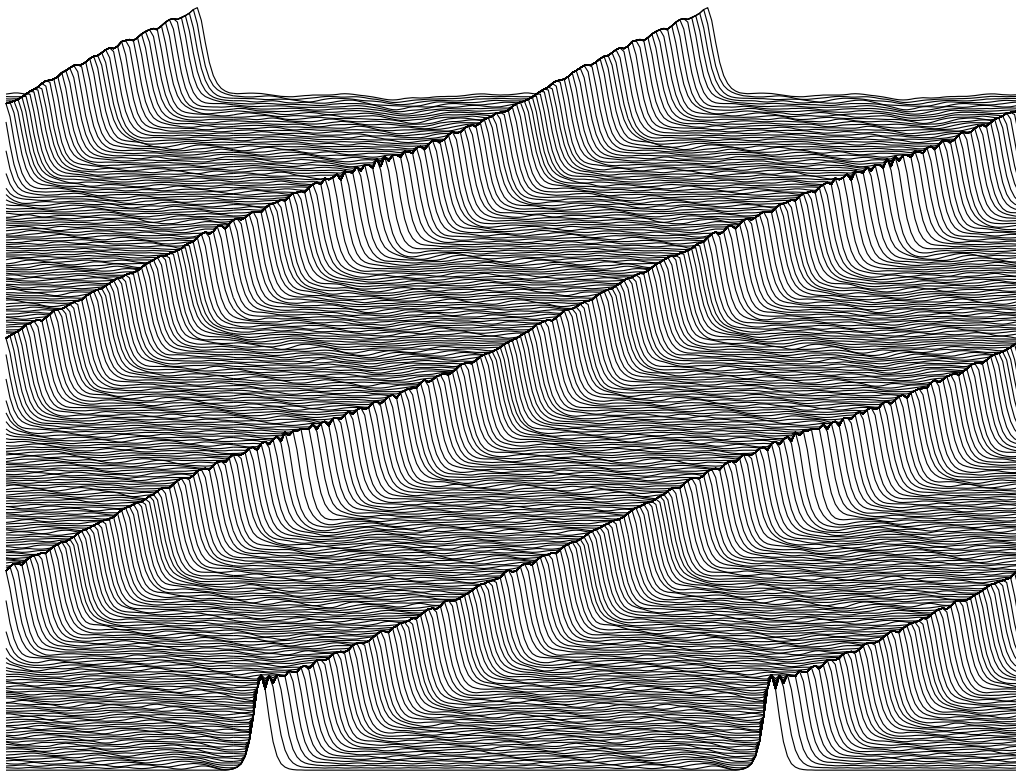


Fig. 18. Third solution type. Propagation of initial excitation (4), amplitude $A=2.03$, $d_I=2.0$ and $b_I=4.0$ and $t_f=300$, $n=128$.

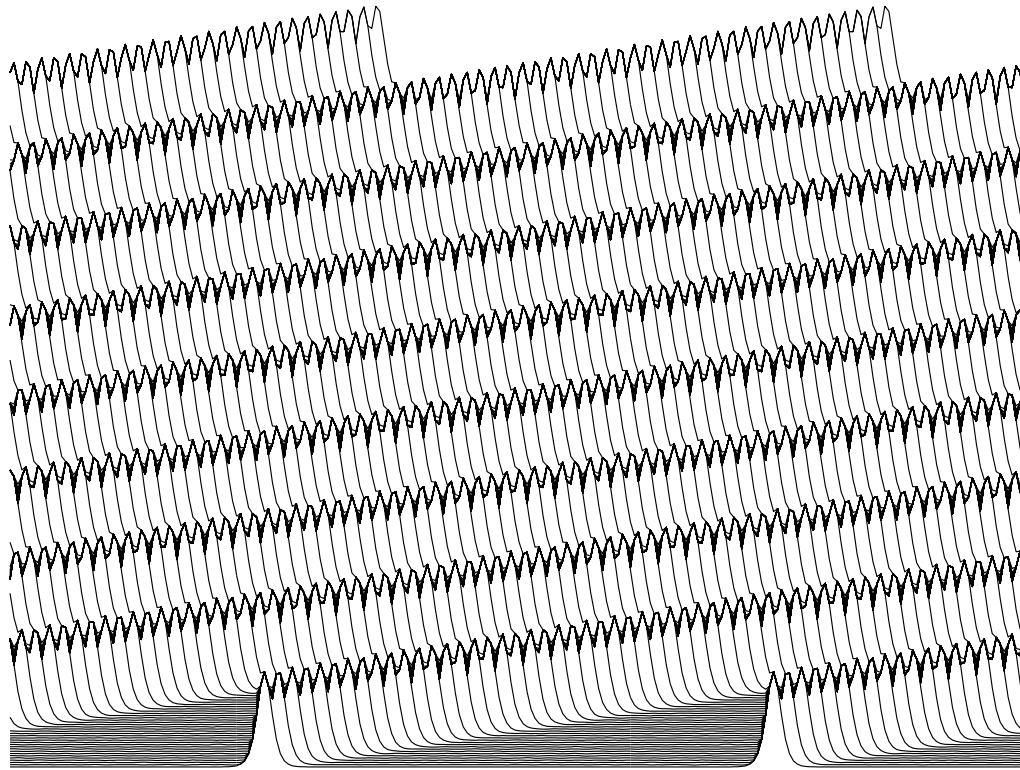


Fig. 19. Third solution type. Propagation of initial excitation (4), amplitude $A=2.09$, $d_I=2.0$ and $b_I=4.0$ and $t_f=300$, $n=128$.

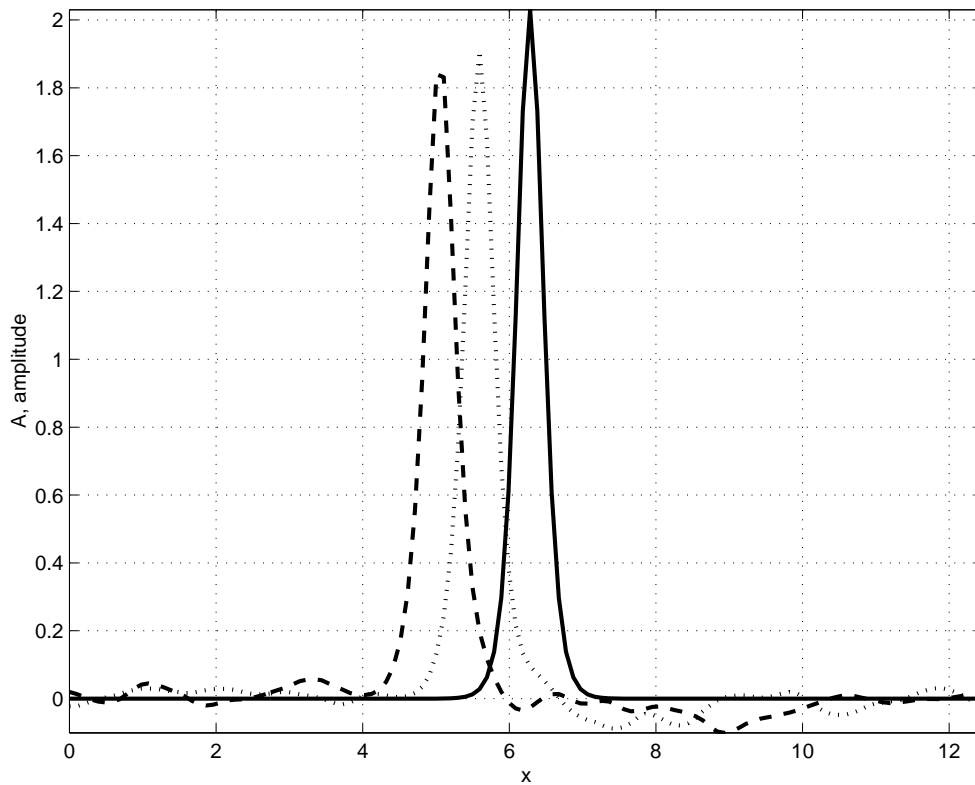


Fig. 20. Third solution type. Wave profiles of the solution, case $d_I=2.0$, $b_I=4.0$ and $A=2.03$. Solid line corresponds to time moment $t=0$, dotted line corresponds to time moment $t=100$ and dashed line corresponds to time moment $t=200$.

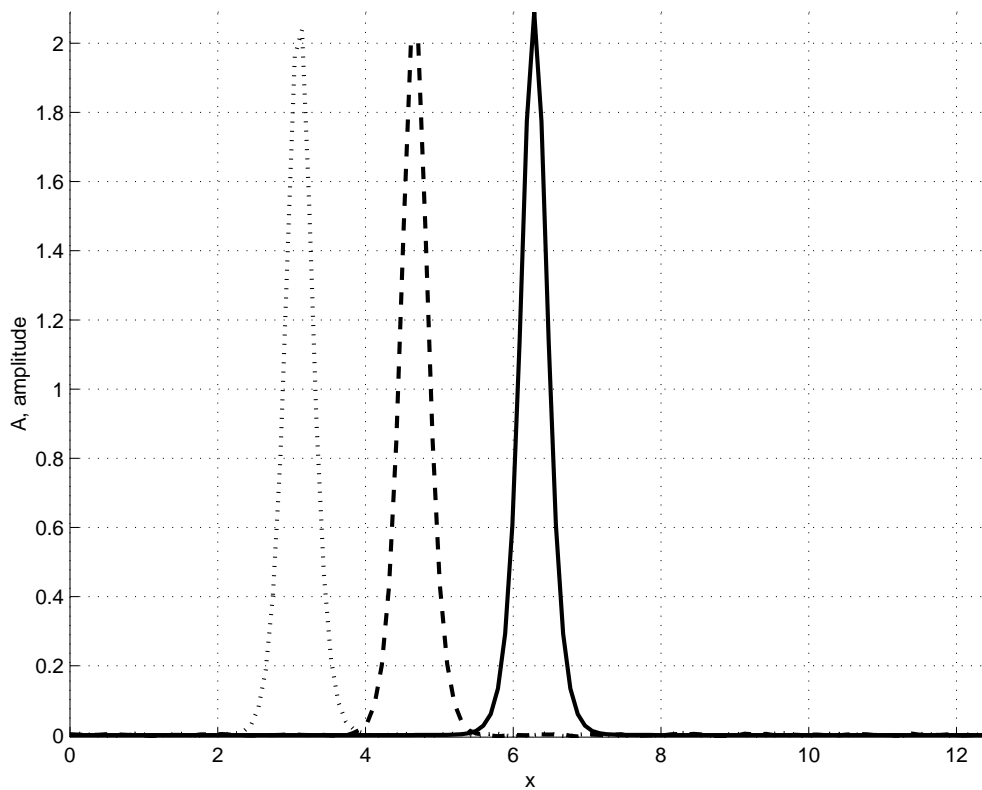


Fig. 21. Third solution type. Wave profiles of the solution, case $d_I=2.0$, $b_I=4.0$ and $A=2.09$. Solid line corresponds to time moment $t=0$, dotted line corresponds to time moment $t=100$ and dashed line corresponds to time moment $t=250$.

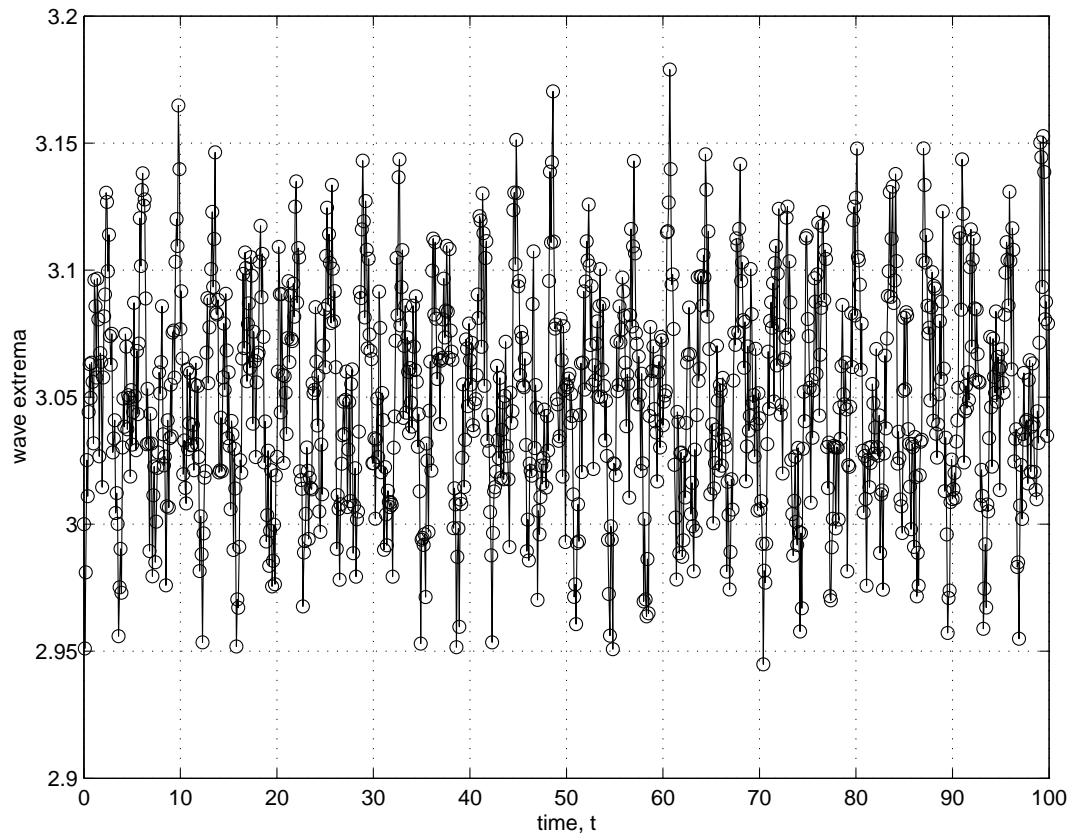


Fig. 22. Third solution type. Maxima of the wave profiles of the solution against time, case $d_I=0.8$, $b_I=1.2$ and $A=3.0$.

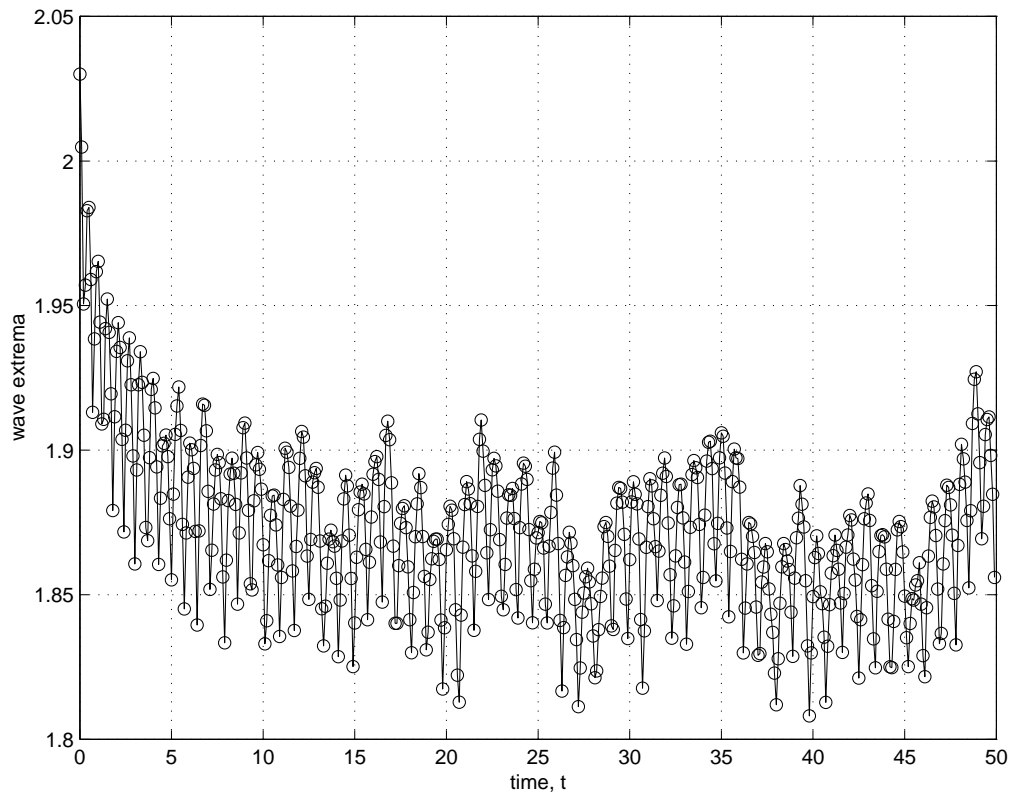


Fig. 23. Third solution type. Maxima of the wave profiles of the solution against time, case $d_l=2.0$, $b_l=4.0$ and $A=2.03$.

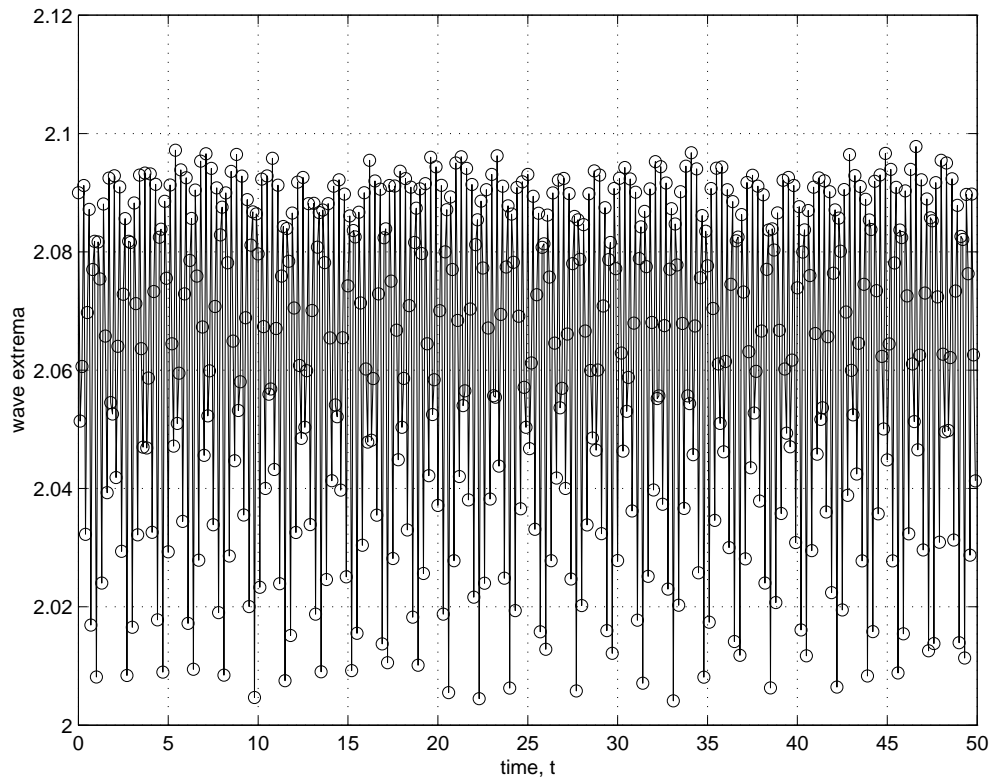


Fig. 24. Third solution type. Maxima of the wave profiles of the solution against time, case $d_l=2.0$, $b_l=4.0$ and $A=2.09$.

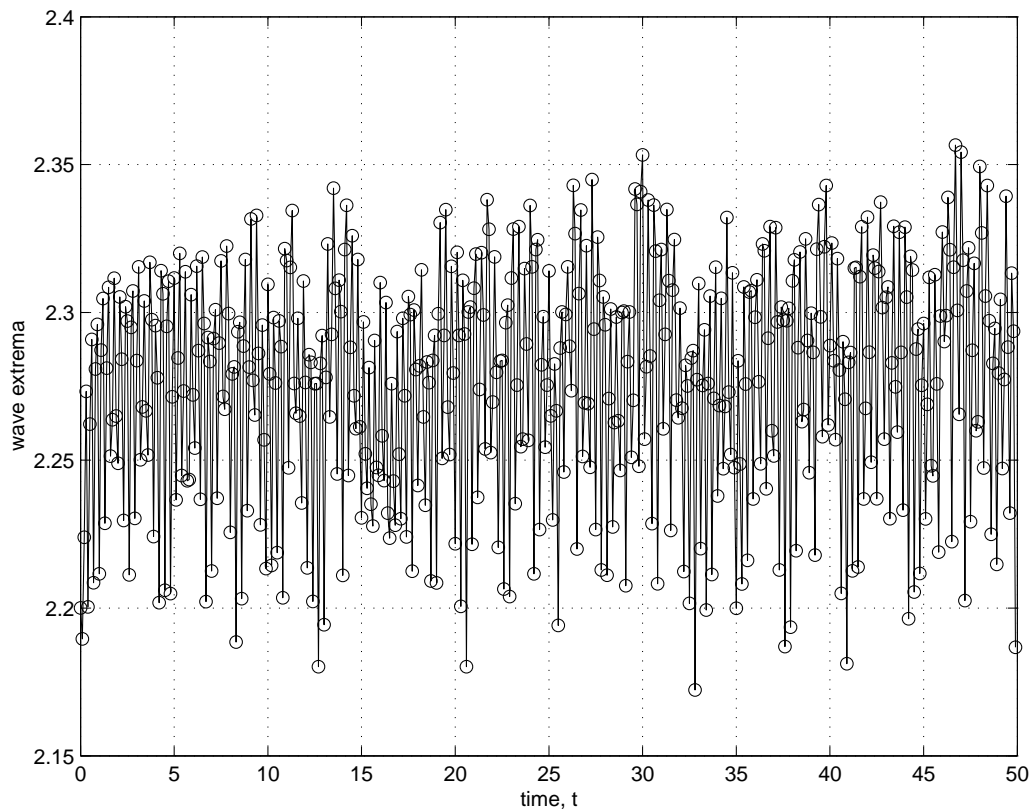


Fig. 25. Third solution type. Maxima of the wave profiles of the solution against time, case $d_l=2.0$, $b_l=4.0$ and $A=2.20$.

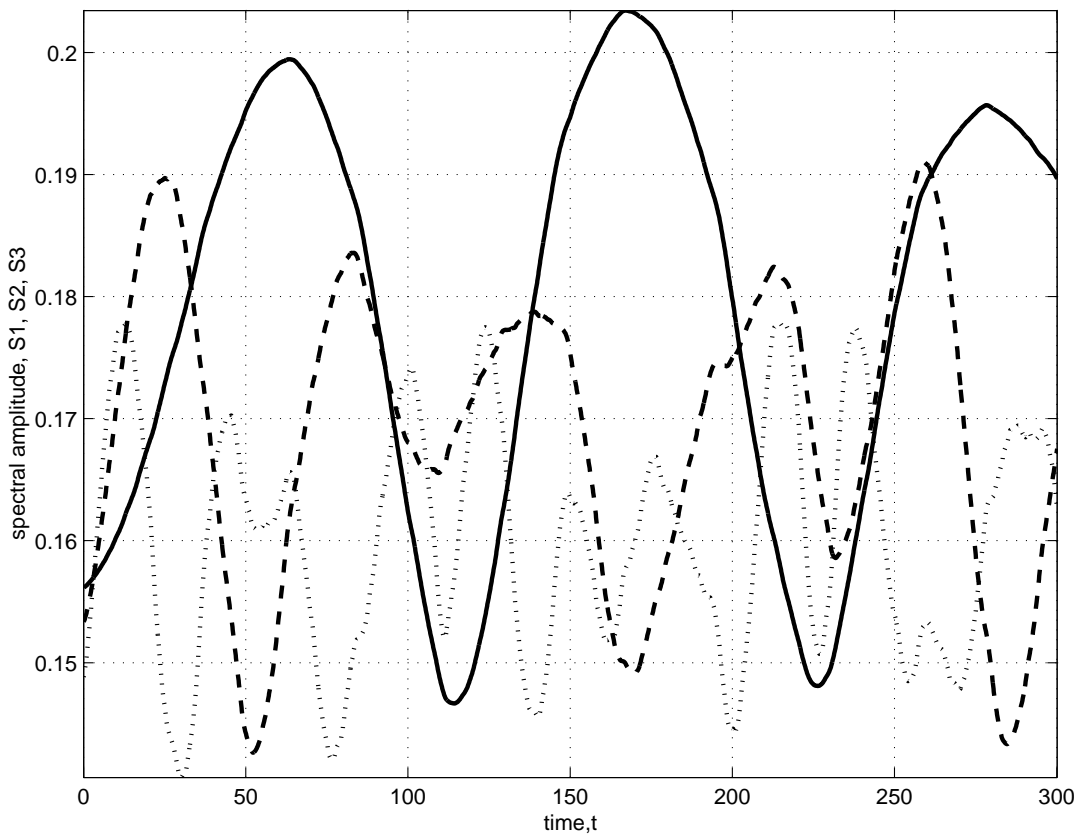


Fig. 26. Third solution type. First three spectral amplitudes S_1 , S_2 , S_3 against time; case $A=2.03$, $d_l=2.0$ and $b_l=4.0$ (solid line corresponds to S_1 , dashed line to S_2 and dotted line to S_3).

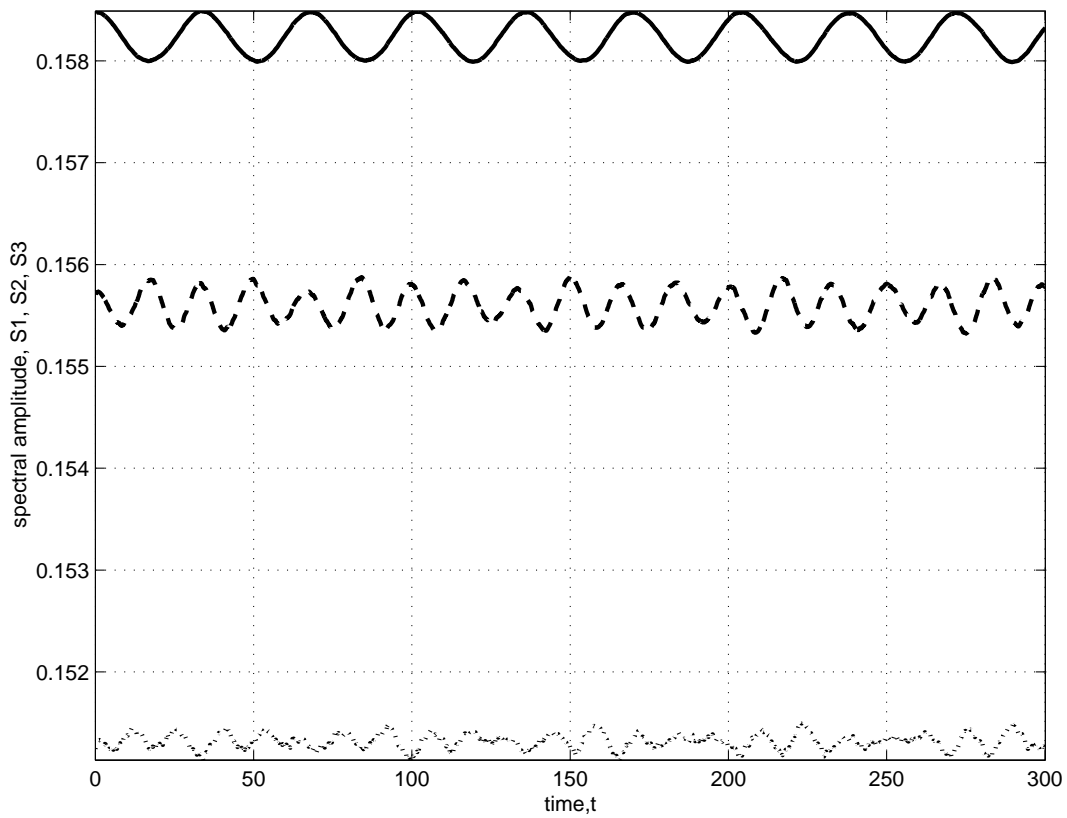


Fig. 27. Third solution type. First three spectral amplitudes S_1 , S_2 , S_3 against time; case $A=2.09$, $d_l=2.0$ and $b_l=4.0$ (solid line corresponds to S_1 , dashed line to S_2 and dotted line to S_3).

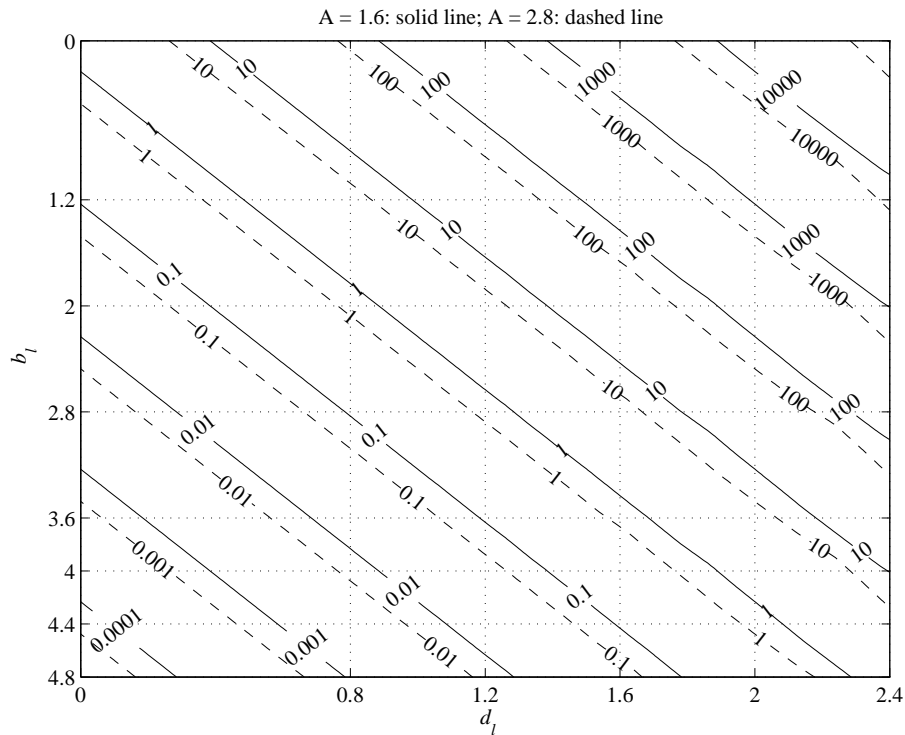


Fig. 28. Ratio r_d against logarithmic dispersion parameters d_l and b_l for amplitudes $A=1.6$ (solid line) and $A=2.8$ (dashed line). Gridlines correspond to cells in Table 1.

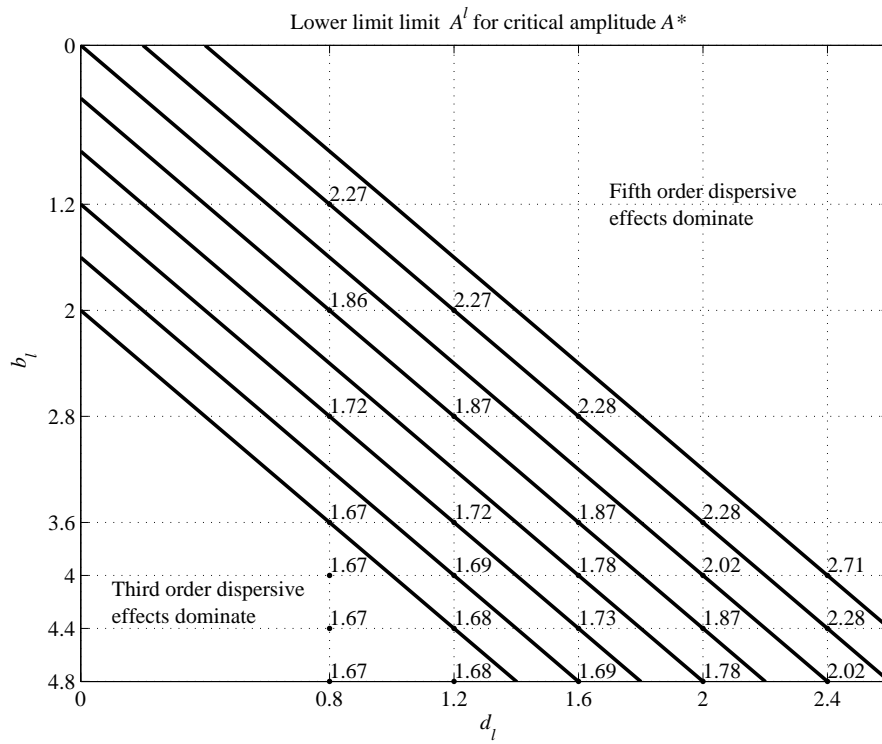


Fig. 29. Lower limit A^l for critical amplitude A^* against logarithmic dispersion parameters d_l and b_l .

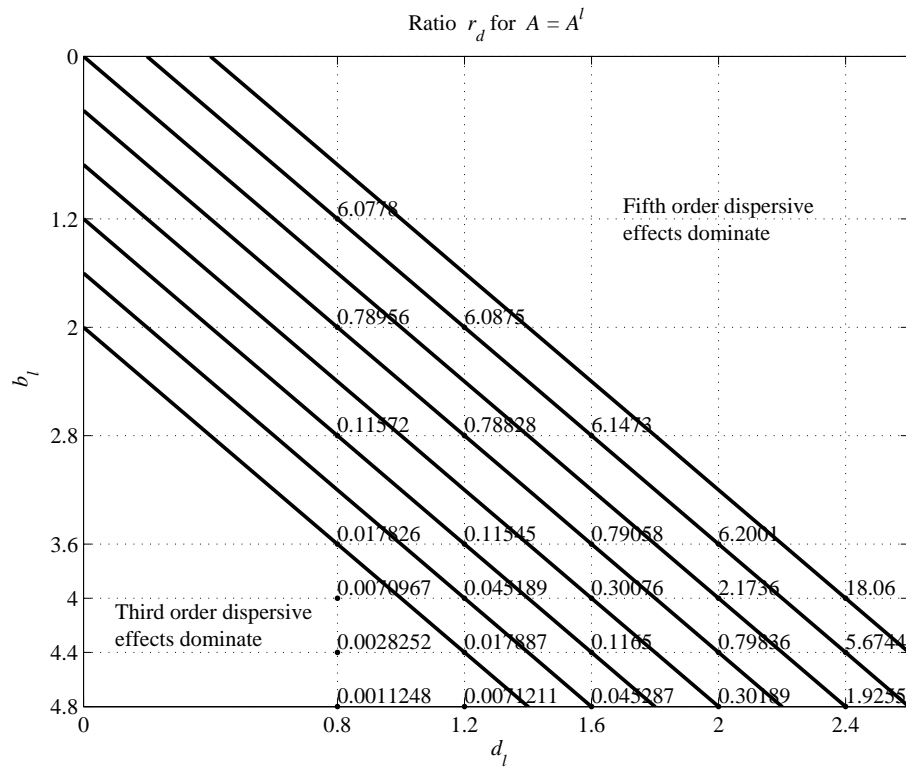


Fig. 30. Ratio r_d against logarithmic dispersion parameters d_l and b_l .

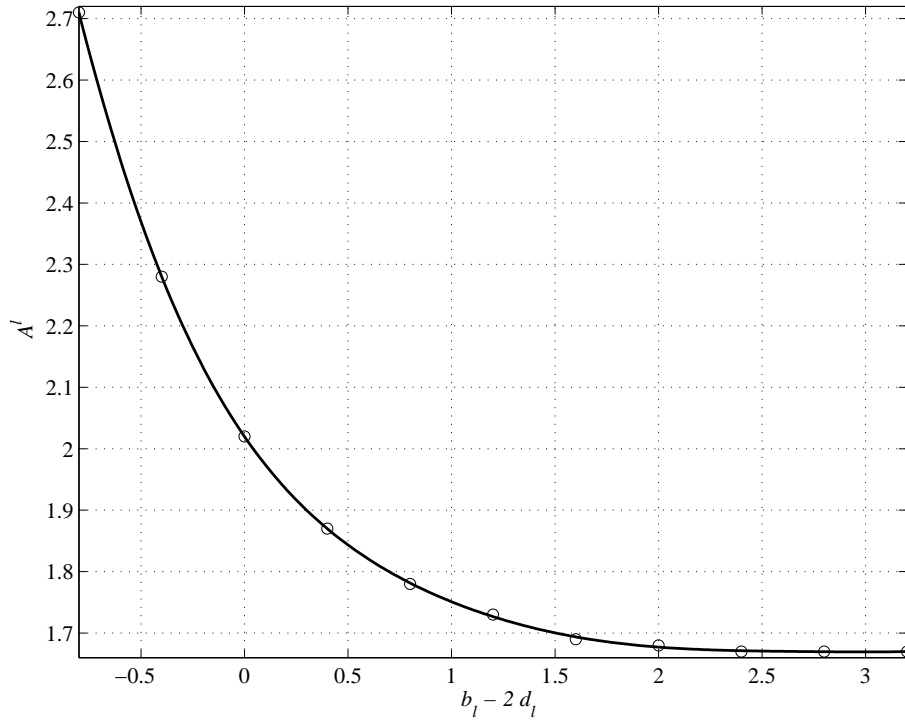


Fig. 31. Lower limit A^l for critical amplitude A^* against quantity $b_1 - 2d_1$.



Fig. 32. Interaction of two solitons, case $d_1=1.6$, $b_1=2.8$; $A_1=2.73$, $A_2=2.90$ and $t_f=300$.

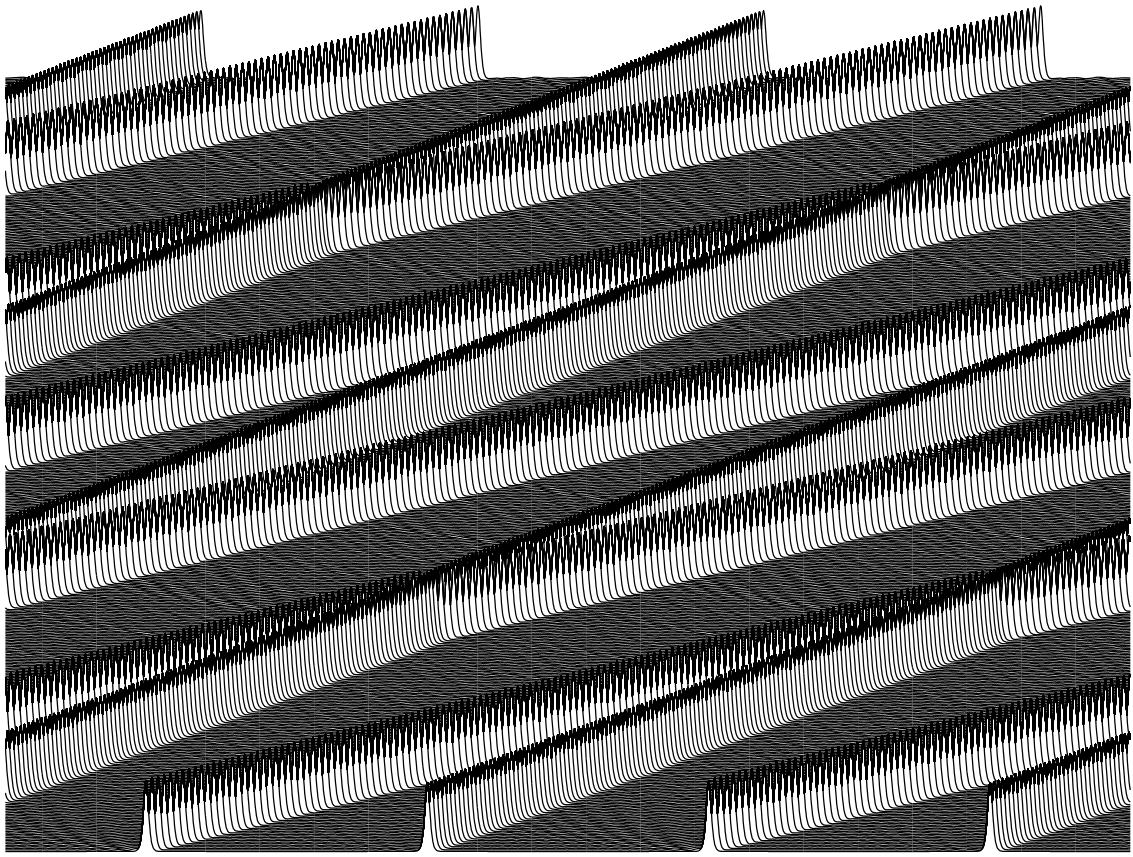


Fig. 33. Interaction of two solitons, case $d_I=2.4$, $b_I=4.8$; $A_1=2.08$, $A_2=2.12$ and $t_f=300$.

8. References

1. **Abe, K., Abe, T.**, *Recurrence of initial state of the Korteweg-de Vries equation*. Phys. Fluids 22 (9), 1644-1646, 1979
2. **Bracewell, R. N.** *The Fast Fourier Transform and Its Applications*. McGraw-Hill, New York, 1978.
3. **Fornberg, B.A.** *Practical Guide to Pseudospectral Methods*. Cambridge University Press, Cambridge, 1998.
4. **Goda, K.** *Numerical Studies on recurrence of the Korteweg-de Vries equation*. J. Phys. Soc. Japan, 42(3), 1040-1046, 1977.
5. **Kreiss, H.-O., Olinger, J.** *Comparison of accurate methods for the integration of hyperbolic equations*. Tellus, 24, 199-215, 1972.
6. **Maugin G.A., Christov C.** *Nonlinear duality between elastic waves and quasi-particles in microstructured solids*. Proc. Estonian Acad. Sci. Phys.Math., 46, 78–84, 1997
7. **Maugin, G.A.** *Material Inhomogeneities in Elasticity*. Chapman & Hall, London et al., 1993.
8. **Salupere, A.** *On the application of pseudospectral methods for solving nonlinear evolution equations and discrete spectral analysis*. In Proc. of 10th Nordic Seminar on Computational Mechanics. Tallinn, 76-83, 1997.
9. **Salupere, A.** *On the application of the pseudospectral method for solving the Korteweg-de Vries equation*. Proc. Estonian Acad. Sci. Phys. Math. 44, 1, 73-87, 1995.
10. **Salupere, A., Engelbrecht, J., Maugin, G.A.** *Solitonic structures in KdV-based higher order systems*. Wave Motion, 34, 51–61, 2001.
11. **Salupere, A., Maugin, G.A., Engelbrecht, J., Kalda, J.** *On the KdV soliton formation and discrete spectral analysis*. Wave Motion 23/1, 49-66, 1996.
12. **Zabusky, N.J., Kruskal, M.D.** *Interaction of solitons in a collisionless plasma and the recurrence of initial states*. Phys. Rev. Lett., 15, 240-243, 1965.